Atmospheric Research 294 (2023) 106987

Contents lists available at ScienceDirect

Atmospheric Research

journal homepage: www.elsevier.com/locate/atmosres

Moisture sources and climatic effects controlling precipitation stable isotope composition in a western Mediterranean island (Pianosa, Italy)

Stefano Natali [a,b,c,*], Marco Doveri [c], Linda Franceschi [b,c], Roberto Giannecchini [b,c,e], Marco Luppichini [b], Matia Menichini [c], Giovanni Zanchetta [b,d,e]

[a] Department of Earth Sciences, University of Florence, via G. La Pira 4, 50121 Florence, Italy
[b] Department of Earth Sciences, University of Pisa, via S. Maria 53, 56126 Pisa, Italy
[c] Institute of Geosciences and Earth Resources, IGG-CNR, via Moruzzi 1, 56124 Pisa, Italy
[d] Institute of Environmental Geology and Geoengineering, IGAG-CNR, 00015 Montelibretti, Rome, Italy
[e] Centre for Climatic Change Impact, CIRSEC, University of Pisa, Pisa, Italy

ARTICLE INFO

Keywords:
Monthly precipitation
Stable isotopes
Deuterium excess
Backward trajectories
Moisture uptake

ABSTRACT

The Mediterranean basin is indicated as a hot spot of climate change, which is an area whose climate is especially responsive to variations. The insular environment is one of the most threatened by the current climate change, especially in terms of drought events, with serious consequences for water scarcity and water stress. This issue is even enhanced in small islands, whose ecosystems are among more sensitive to climatic changes and water availability. The stable isotope composition of hydrogen (δ^2H) and oxygen ($\delta^{18}O$) in precipitation is globally recognized as a powerful natural tracer in the water cycle and represents the starting point to investigate hydrological processes. The understanding of the prevailing factors that drive the isotopic variability of precipitation in the Mediterranean is therefore essential to unravel the hydrological processes and to ensure proper and sustainable management of potentially vulnerable resources to climate change. Here, we discuss the results of multi-year isotopic monitoring in the period 2014–2021 of monthly precipitation collected on Pianosa Island (Italy), a small island located in the northern Tyrrhenian (western Mediterranean). The lower slope and intercept of the Local Meteoric Water Line of the island compared to the Global Meteoric Water Line indicated warmer and drier climatic conditions, suggesting the existence of sub-cloud evaporation processes of raindrops during precipitation, especially in summer. The mean $\delta^{18}O$ of precipitation was lower with respect to other sites placed at higher elevation in this Mediterranean region, due to the lack of summer precipitation which were generally enriched in heavy isotopes. Temperature and amount effects may explain part of the $\delta^{18}O$ variability observed at the monthly and seasonal scale. An HYSPLIT-based moisture uptake analysis indicated the area between the western Mediterranean basin, Italy, and the Adriatic Sea as the region that supplied most of the humidity associated with monthly precipitation samples on Pianosa Island. Less moisture was picked from the northwestern areas of Europe, the North Atlantic Ocean, the proximal Atlantic Ocean, the Iberian Peninsula and North Africa. Consistently with the rainout effect, the higher the moisture fraction picked from the more proximal regions, the more positive the $\delta^{18}O$ of precipitation occurring on Pianosa Island; conversely, the higher the percentage of moisture sourced from more distal regions, the more negative the $\delta^{18}O$. A multiple linear model was proposed to predict the $\delta^{18}O$ of monthly precipitation from temperature, precipitation amount and moisture origin data, which explained 45% of the $\delta^{18}O$ variability. The deuterium excess variability on the island was partly controlled by the local climatic variables, whose effect potentially modifies the original d-excess signature imprinted at the moisture source. No relationship was found between the precipitation deuterium excess and moisture sources, suggesting that more attention should be paid when using the deuterium excess as a tracer of moisture origin, especially in the Mediterranean.

* Corresponding author at: Department of Earth Sciences, University of Florence, via G. La Pira 4, 50121 Florence, Italy.
E-mail address: stefano.natali@unifi.it (S. Natali).

https://doi.org/10.1016/j.atmosres.2023.106987
Received 2 May 2023; Received in revised form 20 July 2023; Accepted 28 August 2023
Available online 30 August 2023

1. Introduction

Both present observations and projections of future climate conditions point out as changes are ongoing or will occur in several regions worldwide in terms of higher temperature, modifications in the seasonal distribution and amount of precipitation, variation of hydro-climatic regimes, increase of frequency, duration and intensity of extreme events, up to shifts in climate types (Bates et al., 2008; Blöschl et al., 2019; Chan and Wu, 2015; Hirabayashi et al., 2013; Milly et al., 2005; Trenberth, 2011; Turco et al., 2015). This scenario has important socio-economic implications (European Environment Agency, 2019), especially for the planning of proper land and water resources management. The Mediterranean basin is indicated as a hot spot of climate change (Giorgi, 2006), which is an area whose climate is especially responsive to changes. A warming trend has been found in the Mediterranean area in the last century (Brunet et al., 2006; Brunetti et al., 2006; Giorgi, 2002), with sharp warming and an increase in high temperature events in summer (IPCC, 2007). Climate projections also point at substantial warming, especially in the warm season (Coppola and Giorgi, 2010; Giorgi and Lionello, 2008; IPCC, 2007). Moreover, negative precipitation trends have been revealed in the Mediterranean in recent decades (Caloiero et al., 2011; Homar et al., 2010; IPCC, 2007; López-Moreno et al., 2010; Norrant and Douguédroit, 2006; Toreti et al., 2010), mostly due to a significant decrease in winter and spring (Hoerling et al., 2012). However, in many areas precipitation trends are not always clear and significant (Alpert et al., 2002; Reale and Lionello, 2013; Xoplaxi, 2002).

The insular environment often represents one of the most threatened by climate change, especially in terms of drought events, with severe consequences for water scarcity and water stress (Giorgi, 2006; Mathbout et al., 2021; Turco et al., 2015). This issue is enhanced in small islands. There are thousands of small islands worldwide, for which the occurrence of freshwater, as well as the water availability for the biosphere, have to be considered in a very precarious equilibrium (Unesco, 1991). In this context, the first step to face these problems is certainly the knowledge of the hydrological processes occurring in the most sensitive environments, in order to obtain a long-term hydrological perspective which allows for the planning of proper and sustainable management of potentially vulnerable resources to climate change. Ensuring a reliable and sustainable water supply through effective water resource planning depends on our ability to understand hydrological flows and their variability in the future (Gusyev et al., 2016; Watanabe et al., 2018).

Precipitation represents the first step of the water cycle and the input for all the surface and sub-surface processes. The stable isotopic composition of hydrogen (δ^2H) and oxygen ($\delta^{18}O$) in precipitation is globally recognized as a powerful natural tracer in the water cycle (Bowen et al., 2019; Clark and Fritz, 1997; Dansgaard, 1964; Gat, 1996; Gat et al., 2001) and represents the starting point to investigate hydrological processes. The precipitation isotope composition is also widely adopted to characterize the regional atmospheric patterns (Baldini et al., 2008; Comas-Bru et al., 2016; Zhao et al., 2022), to understand groundwater recharge mechanisms and dynamics (Jasechko, 2019), and to investigate water uptake and movement in natural ecosystems and agroecosystems (Amin et al., 2020; Penna et al., 2018). In the Mediterranean region, few comprehensive investigations have been performed to analyze the statistical relationships between stable isotopes of oxygen and hydrogen in precipitation and climatic variables (Giustini et al., 2016; Longinelli and Selmo, 2003; Natali et al., 2021; Rindsberger et al., 1983). Moreover, most of the studies on isotope hydrology of precipitation in the western Mediterranean (e.g., Doveri et al., 2019; Frot et al., 2007; Giustini et al., 2016; Longinelli and Selmo, 2003) lack thorough investigations aimed to define the origin of precipitation and the relationship between moisture origin and rainfall isotopic composition, except for a few (Casellas et al., 2019; Cruz-San et al., 1992; Dumitru et al., 2017; Liotta et al., 2008; Moreno et al., 2014). Hence, the understanding of the prevailing factors that drive the seasonal and annual cycles in $\delta^{18}O$, δ^2H and d-excess of precipitation is a challenging task in the Mediterranean to better define the climatic controls on the $\delta^{18}O$ and δ^2H and processes affecting the hydrological cycle in the region, including on islands.

In this work, we present and discuss the results of multi-year isotopic monitoring of monthly precipitation collected on Pianosa Island, a small island located in the northern Tyrrhenian Sea (Tuscan Archipelago) between Corsica and the shoreline of Tuscany (Central Italy). Pianosa hosts aquifers with significant groundwater resources, albeit its small extension, flat morphology, and climatic regime characterized by low precipitation (Doveri et al., 2012), which is typical of the Mediterranean. In the past (70s and 80s of the last century), this groundwater resource represented the main source of water supply for over 1500 people when the penitentiary, still present on the island, was at its peak. However, the likely overexploitation of the aquifer, enhanced by agricultural and livestock activities, determined a quantitative and qualitative deterioration over time due to pollution and seawater intrusion (Doveri et al., 2012). Hence, investigations on the water cycle and hydrological processes in the present day are required on Pianosa Island, especially under the current scenario of a changing climate.

A total of 73 monthly precipitation samples were collected on the island from October 2014 to December 2021, and they were analysed for $\delta^{18}O$ and δ^2H aiming to the following objectives: 1) to define the Local Meteoric Water Line (LMWL) of Pianosa Island, evaluating the atmospheric processes that influence precipitation isotopic composition on this island in the Tyrrhenian Sea; 2) to define climatic controls on the isotope signatures of precipitation, at monthly, seasonal, and annual scale; 3) to reconstruct backward trajectories for each monthly precipitation sample collected from 2015 to 2021 and to evaluate the potential influence of moisture uptake locations on the isotopic composition of precipitation; 4) to propose a multivariate linear model for predicting the $\delta^{18}O$ in precipitation by temperature, precipitation amount and moisture origin data. Results from this work provide the basis for further hydrological, hydrogeological and paleoclimatic investigations on Pianosa Island.

2. Study area and climate

Pianosa Island (42°35′07" N, 10°04′44′ E) is located in the middle of the northern Tyrrhenian Sea (Fig. 1A), in the western Mediterranean basin. It is placed about 13 km southeast of Elba Island, about 45 km east of Corsica and about 55 km west of the shoreline of Tuscany. Pianosa is the fifth largest among the islands of the Tuscan Archipelago, which also includes the islands of Elba, Giglio, Capraia, Montecristo, Gorgona, Giannutri and other smaller islets, and with a surface of 10.3 km^2 and a coastal perimeter of 18 km. Pianosa differs from other hilly-mountainous islands for its typically flat morphology, with an average altitude of 18 m a.s.l. and a maximum elevation that reaches 29 m a.s.l. in the northern sector. The island has a sub-triangular shape (Fig. 1B): the southern part has an *E*-W width of just over 4.5 km, whereas the northern part consists of a very narrow and elongated promontory of about 3 km.

Pianosa is characterized by a particular climate due to its position in the Tyrrhenian Sea and its flat morphology, which distinguishes it from the other islands of the Tuscan Archipelago. According to Köppen's classification system (Köppen, 1931), the climate is explained as Csa. Precipitation is rather low with a mean annual value of 481 mm, as calculated by instrumental time series measured from 1951 to 2007 at the meteorological station on the island (Fig. 1B), managed by the LaMMA Consortium - Environmental Modelling and Monitoring Laboratory for Sustainable Development (http://www.lamma.rete.toscana.it/) (Nicotra, 2008). The small size of the island and the absence of reliefs limit the condensation of moist air masses. The rainiest season is autumn, with the maximum rainfall in October, whereas summer is the driest one with a minimum in July. The atmospheric temperature follows the typical trend of the Mediterranean area, with higher values in

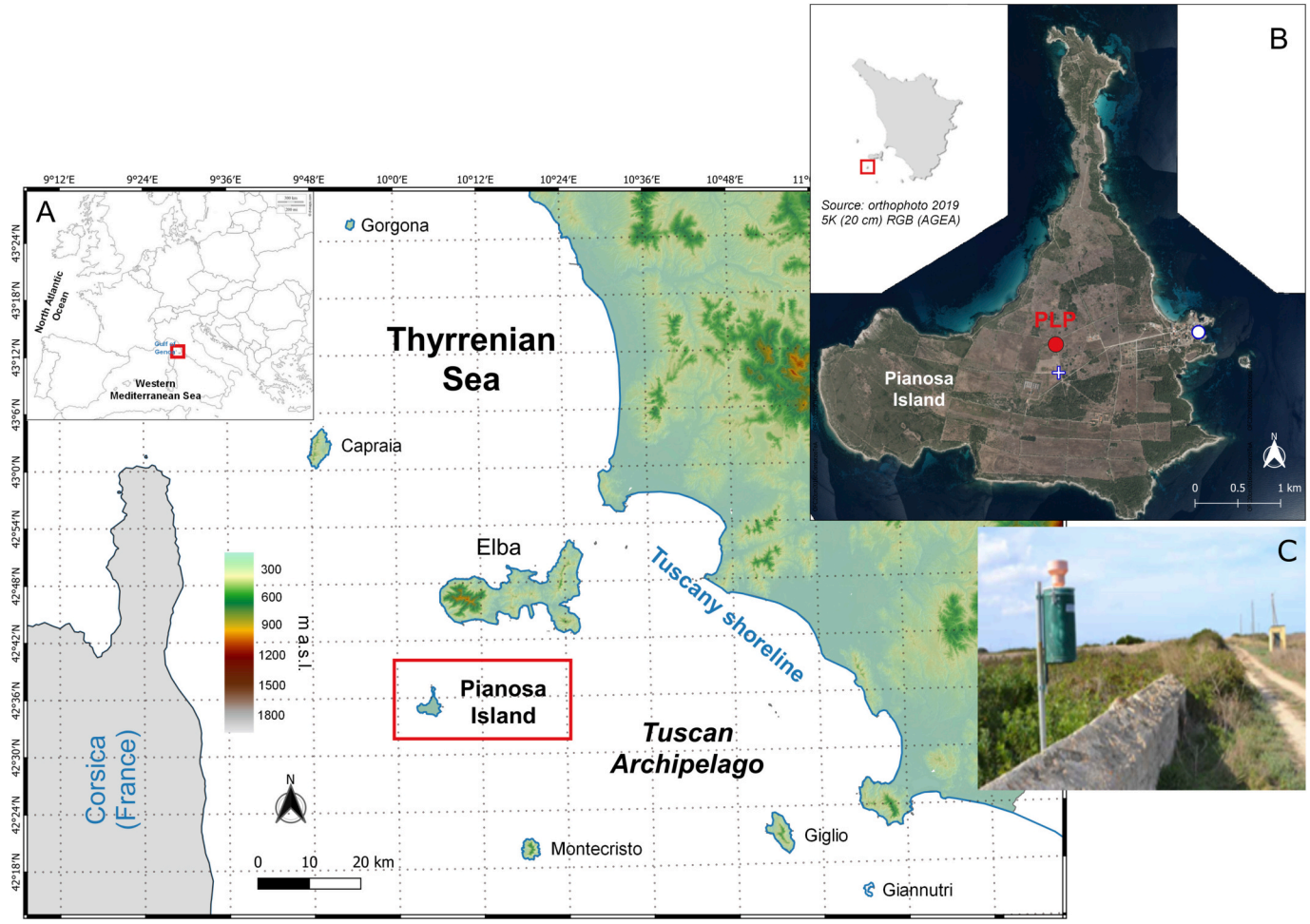

Fig. 1. Map of the study area. A) Location of Pianosa Island in the Thyrrenian Sea (western Mediterranean); B) Orthophoto of the island showing the typical flat morphology. The thermometer/barometer in situ is indicated by the white cross. The white circle indicates the LaMMA Consortium meteorological station; C) Precipitation collector used to collect monthly precipitation.

summer and lower values in winter. Monthly mean temperature ranges from a minimum in January/February to a maximum in July/August, with an average annual temperature of 14.4 °C. The autumn temperatures are on average higher than the spring ones, probably due to the large influence of the sea on climate, with consistent heat releases from the sea surface to the atmosphere.

From a geological point of view, Pianosa Island is entirely made up of sedimentary rocks. The outcropping lithotypes are mostly Plio-Pleistocene marine organogenic calcarenites and cemented sands, lying on a Miocene sedimentary succession (marl and clay with interbedded conglomerate). The series ends with marine and continental Quaternary deposits (Foresi et al., 2000; Raggi, 1983). The permeability of these outcropping sedimentary rocks, along with the flat morphology and the absence of a surface hydrographic network, promotes the infiltration of precipitation water. As a consequence of these characteristics, the island has important aquifers with significant groundwater resources, albeit its small extension and low precipitation (Doveri et al., 2012). Since the presence of rocks with a carbonate component, karst processes are significant on the island, which occur with both epigean (e.g. dolines) and underground forms (caves and tunnels with a prevalently horizontal development). The most important underground forms currently known are the Cervo Cave and the Lancia Cave, along the eastern coast of the north sector of the island, in which some speleothems (stalactites, stalagmites and flowstones) are present (our observation). Karst processes have important implications on the hydrogeological setting of the island, ensuring a high infiltration potential of precipitation that feeds the groundwater systems.

3. Materials and methods

3.1. Precipitation monitoring, samples collection and meteorological data

An isotopic monitoring of precipitation was carried out on Pianosa Island from October 2014 to December 2021, as part of different projects coordinated by the Institute of Geosciences and Earth Resources of the National Research Council (IGG-CNR) and the Earth Science Department of the University of Pisa (DST-UNIPI), and partly funded by the Province of Livorno and the Tuscan Archipelago National Park. A total of 81 monthly precipitation samples were collected also thanks to the collaboration with the penitentiary police of the island. 73 monthly precipitation samples were analysed of the total collected samples, as 8 precipitation samples were discarded due to very low amounts (<2 mm, Table A.1, supplementary materials). Isotopic data of monthly precipitation collected from 2014 to 2018 are included in the regional isotopic database published by Natali et al. (2021) and were used for the definition of the LMWL of Tuscany (Natali et al., 2021). However, these data have only been discussed as a whole and no detailed evaluation of climatic controls on the precipitation isotope composition on Pianosa Island was performed. The monitoring station (named PLP) was located in the centre of the island (42°35′9″N, 10°4′44″E) at an altitude of 19 m a.s.l. (Fig. 1B). Homemade oil collector was adopted to collect monthly precipitation (Fig. 1C), equipped with a 10 L bottle and a funnel of 16

cm. A thin layer of paraffin oil (ca. 0.3 L) was added to bottles before each sampling period to prevent evaporation. Oil was accurately separated by using separatory funnels (IAEA, 2014), to avoid the presence of oil fractions in the water samples that can create various issues for laboratory analysis. The bottle was changed at the end of each month, typically between the last day of the month and the first day of the following one. The total precipitation amount during each month was measured by subtracting the initial weight of the bottle with oil from the final weight. Free-oil aliquots were therefore filtered through 0.45 μm nylon filters and transferred in 50-mL double-sealing HDPE bottles and stored at a temperature of about +4 °C before the analysis.

Hourly air temperature was measured over the investigation period using a Diver Baro probe (Schlumberger Water Services) with an accuracy of ±0.1 °C (Fig. 1B) which was placed very close to the rain collector.

3.2. Isotopic analysis

Samples collected from October 2014 to December 2020 were analysed at the IGG-CNR of Pisa; samples collected from January 2021 to December 2021 were analysed at the Laboratory of Fluid Geochemistry (LFG) of the University of Florence. Different isotopic techniques and equipment were used at two laboratories, and some tests were performed by analysing internal standards and reference materials to verify the congruence of isotopic measurements. A few real samples were also analysed by more techniques to check the comparability of measurements. Oxygen isotope composition was measured at IGG-CNR by the water-CO_2 equilibration technique (Epstein and Mayeda, 1953) followed by the analysis of CO_2 using a Finnigan MAT 252 mass spectrometer (IRMS). A Los Gatos Research (LGR) Liquid Water Isotope Analyzer based on the "Off-Axis Integrated Cavity Output Spectroscopy" technique (Lis et al., 2008) was used at IGG-CNR to determine the hydrogen isotope composition. $\delta^{18}O$ data from LGR were not used because of some randomly distributed errors that were detected during the analyses of secondary standard and replicated samples. On the contrary, laboratory tests revealed that $\delta^{2}H$ data from LGR were more consistent than the IRMS method and characterized by high reproducibility. The $^{18}O/^{16}O$ and $^{2}H/H$ isotopic ratios of the other samples were determined at LFG using a Picarro L2130-i analyzer based on cavity ring-down spectroscopy (CRDS). Picarro's ChemCorrect post-processing software was used to analyze the spectral features of samples and to determine whether the analysis was compromised by organic molecules (e.g., paraffin oil). The data are expressed as δ‰ compared to the international reference standard V-SMOW. The total error was within ±0.1 ‰ for $\delta^{18}O$ and ± 1 ‰ for $\delta^{2}H$ for all methods. All the laboratories ran isotopic reference materials spanning isotope scales of interest which were calibrated to the VSMOW-SLAP scale. An internal lab standard was run several times among samples as a check on the instrumentation. d-excess was calculated by Dansgaard's equation (Dansgaard, 1964) using the relationship d-excess = $\delta^{2}H - 8*\delta^{18}O$. Error propagation for d-excess was calculated according to the formula proposed by Natali et al. (2022), and it resulted in an error of about ±1.8 ‰, by using the total errors of ±0.1 ‰ for $\delta^{18}O$ and ± 1 ‰ for $\delta^{2}H$.

3.3. Backward-trajectory and moisture sources diagnostic

To diagnose the origin and pathways of precipitating air masses and to better understand the rainfall isotopic variability in this island of the western Mediterranean, we reconstructed the moisture uptake regions of each monthly precipitation sample by applying back-trajectory analysis. The Hybrid Single-Particle Lagrangian Integrated Trajectory (HYSPLIT) model of the Air Resources Laboratory (ARL) of the National Oceanic and Atmospheric Administration (NOAA) (Rolph et al., 2017; Stein et al., 2015) was used to identify the pathways of moist air masses at the precipitation sampling site in the period 2015–2021. All calculations were performed through PySPLIT (Warner, 2018), which is a Python-based Application Programming Interface (API) for HYSPLIT. The necessary input data for this model consists of gridded meteorological data, a location, a starting altitude of the model, a runtime, and a starting date. Global Data Assimilation System (GDAS1) grids were used as meteorological input data, with a horizontal resolution of 1° (ca. 111 km) and 23 vertical layers (available at ftp://arlftp.arlhq.noaa.gov/pub/archives/gdas1). The archive meteorological data from GDAS1 are provided in UTC (Coordinated Universal Time) time. Therefore, precipitation data registered on the ground in the study area were synchronized to UTC. 5-day (120*h*) back trajectories were initialized at PLP for each month from January 2015 to December 2021. The model runtime of 5 days backward from the time of precipitation was chosen to avoid an increase of uncertainty of trajectories with time, but to be within 10 days, a period that is considered as the average residence time of water vapour in the atmosphere (Numaguti, 1999). Trajectories were initialized at 1500 above ground level (a.g.l.) every 6 h per day (00, 06, 12, 18 UTC) and then only trajectories corresponding at hours with 6 h cumulative precipitation >0 mm were selected, for a total of 1207 5-day back trajectories. 6 h cumulative precipitation values were obtained using the hourly precipitation records registered at the LaMMA Consortium meteorological station on the island. To track the specific air mass producing precipitation at the precipitation monitoring sites, the starting altitude of the model should ideally correspond to the cloud altitude during precipitation. Unfortunately, no radiosonde ascent measurements providing absolute cloud base and humidity maxima were available for the study area over the investigation period. However, most of the moisture in the atmosphere is thought to be in the first 2000 m a.g.l. (Bershaw et al., 2012; Wallance and Hobbs, 2006), and elevations lower than 1000 m a.g.l. should not be considered in order to minimize the influence of surface topography on wind direction. Moreover, back trajectories from different starting altitudes showed similar paths (Baldini et al., 2010; Krklec et al., 2018; Krklec and Domínguez-Villar, 2014). Therefore, we selected the altitude of 1500 m a.g.l. (approximately equivalent to 850 hPa atmospheric level) as the initial vertical height and it was assumed to be representative of the column of air where most of the moisture was contained. The numerical trajectory error was estimated by generating the reversed trajectories that were initialized at the end of the original trajectories and run the opposite direction. By calculating the total travel distance of the two trajectories and the distance between the original trajectory start and reverse trajectory endpoints, we estimated the relative integration error. Only the trajectories with an error lower than 5% were selected and used for further calculations, for a total of 959 5-day back trajectories.

As previously stated by other authors (e.g., Krklec et al., 2018; Sodemann et al., 2008), the modelled air mass trajectories from a site during the days previous to precipitation events could provide erroneous and misleading estimations of the actual moisture sources of those events. Air masses do not uptake moisture along their full trajectory, but only when certain requirements are fulfilled (Sodemann et al., 2008). Consequently, the spatial distributions of back trajectories and moisture uptake locations may be very different. Hence, an additional model is required to identify moisture uptake locations along back trajectories (Baldini et al., 2010; Bershaw et al., 2012; Krklec et al., 2018; Krklec and Domínguez-Villar, 2014; Sodemann et al., 2008). In this study, the identification of moisture uptake locations and the definition of the actual moisture source regions were based on the quantitative diagnostic proposed by Sodemann et al. (2008) and applied in several other studies (e.g., Casellas et al., 2019; Krklec et al., 2018; Oza et al., 2022; Saranya et al., 2021; Wolf et al., 2020). This method relies on the assumption that specific humidity (q, g/kg) changes during a specific time interval (6 h) at a particular trajectory location reflect the effects of evaporation and precipitation along the air mass pathway. To calculate the moisture uptake along each trajectory we used specific humidity data, considering a threshold of the positive gradient in specific humidity of 0.2 g/kg within 6 h (Sodemann et al., 2008). If the change in specific humidity (Δq) of the air parcel between the time 't' and "t-6 h"

was ≥0.2 g/kg, then there was a moisture uptake. If this uptake occurred below the "planetary boundary layer" (PBL, which is defined as the lowest part of the atmosphere whose behaviour is directly influenced by its contact with the planetary surface), the trajectory location was considered as the actual moisture source; conversely, if the uptake occurred above the PBL, the location was discarded because it was not possible to be sure that the moisture was coming from below the air parcel. Moisture uptake locations were therefore identified along each trajectory of each month. To evaluate the influence of the moisture sources on the isotope signal of monthly precipitation we divided the area into regions, a common methodology to evaluate the role of moisture sources on the isotope composition of precipitation (Krklec et al., 2018; Krklec and Domínguez-Villar, 2014; Zhang et al., 2020). 11 regions around the Pianosa Island were defined (Fig. A.1): distal Atlantic (*dA*); north Atlantic (*nA*); north America and Greenland (*nAm_Gr*); proximal Atlantic and Iberian Peninsula (*pA_IP*); north Africa (*nAf*); western Mediterranean and Italy (*wM_It*); eastern Mediterranean (*eM*); southeast (*se*); northeast (*ne*); north (*n*); northwest (*nw*). The geographical limits (e.g., ocean-continent borders) and the spatial distribution of trajectories were considered when defining these regions. For a particular region (*r*) and each month (*m*) in the period 2015–2021, the percentage contribution of moisture uptake (PMU) is estimated following the formula (1):

$$PMU_r\ (\%) = \frac{f_r}{TF} \bullet 100 \quad (1)$$

where f_r is the fraction of moisture (g/kg) picked from the region *r*, which is given by the sum of all Δq of each trajectory within this region, and TF is the total fraction (g/kg) given by the sum of Δq from all the source regions. Besides the percentage contribution of each region, we also calculated the percentage frequency of moisture uptake regions (PFU) following the formula (2):

$$PFU_r\ (\%) = \frac{n_r}{n_{tot}} \bullet 100 \quad (2)$$

where n_r is the total number of points with a valid Δq (≥0.2 g/kg and below the PBL) of each trajectory within a specific region (*r*) and n_{tot} is the total number of points of all the source regions.

3.4. Statistics and calculations

Statistical analyses were performed using R 4.1.2 (R Core Team, 2019) and some packages, including "psych" (Revelle, 2023), "plyr" (Wickham, 2011), "tidyverse" (Wickham et al., 2019), "caret" (Kuhn, 2008), and "QuantPsyc" (Fletcher, 2022). All the standard deviations calculated were given at 1σ. Spearman's rank correlation analysis (Spearman, 1904) was applied between isotopes and hydrometeorological parameters and PMU_r. Correlations were significant for *p*-values <0.05. Moreover, a multiple linear regression was applied to predict the $\delta^{18}O$ of monthly precipitation on the basis of three predictor variables: the monthly mean temperature, the total monthly precipitation amount and an index of the Mediterranean character of each monthly precipitation sample (I_{MED}), as defined in the Subsection 5.4. The multiple linear model was calculated by using the "lm" function in R. The "lm.beta()" function of the package "QuantPsyc" was used to calculate the standardized regression coefficients for each predictor variable and to understand which of these three variables had the greatest influence on the $\delta^{18}O$ of monthly precipitation. Besides arithmetic means, amount-weighted isotopic composition ($\delta^{18}O_w$, δ^2H_w and d-excess$_w$) was calculated using the amount of water (L) measured in the rain collector. Four regression techniques were tested to derive the LMWLs of Pianosa Island. Ordinary least squares regression (OLSR) and reduced major axis (RMA), along with the corresponding precipitation-weighted regressions (PWLSR and PWRMA), were applied (Crawford et al., 2014; Hughes and Crawford, 2012). Precipitation-weighted regressions are useful to minimize the impact of evaporation secondary processes when dealing with small precipitation amounts (Hughes and Crawford, 2012). The root mean of the sum of squared errors (rmSSEav, Crawford et al., 2014) was used to determine the goodness of fit, which is better when rmSSEav equals 1.00.

4. Results

4.1. Climatic conditions

The annual and monthly mean temperatures and precipitation amounts during the monitoring period from 2015 to 2021 are shown in Fig. 2. The mean annual temperature from 2015 to 2021 was 16.5 °C (± 1.1 °C), ranging from a minimum of 14.6 °C in 2021 to a maximum of 17.9 °C in 2018. The total annual mean precipitation was 567 mm (± 122 mm) and ranged from a minimum of 400 mm in 2021 to a maximum of 728 mm in 2016. The mean monthly temperature was 17.5 °C (± 5.6 °C) from October 2014 to December 2021, ranging from a minimum of 8.4 °C in February 2018 to a maximum of 27.9 °C in July 2015. Winter was the coldest season with a mean temperature of 11.2 °C (± 1.4 °C), and January was the coldest month; on the contrary, summer was the warmest season with a mean temperature of 24.8 °C (± 2.1 °C) and August was the warmest month. The maximum monthly precipitation amount was 187 mm in November 2016. Autumn and winter were the rainiest seasons with a mean precipitation of 238 and 164 mm, respectively, and November was the wetter month; precipitation was lower in spring and summer with a mean value of 117 and 48 mm, respectively, and June was the driest month.

4.2. Seasonal and annual isotopic variability of monthly precipitation on Pianosa Island

The $\delta^{18}O$ and δ^2H values of monthly precipitation collected on Pianosa Island from October 2014 to December 2021, the calculated d-excess values, the monthly precipitation amounts, and the monthly mean air temperatures are reported in Table A.1. Summary statistics of raw monthly data from January 2015 to December 2021 are provided in Table 1, whereas the data distribution is shown in Fig. 3 through histograms and boxplots. The isotopic values showed a large variability, which is typical of rainwater. The $\delta^{18}O$ values ranged between −10.5‰ and 0.60‰ with a median value of −5.66‰; the δ^2H values ranged between −69.9‰ and 9.1‰ with a median value of −33.8‰; d-excess ranged between 2.1‰ and 21.7‰ with a median value of 11.6‰.

The isotopic values followed a normal distribution, as shown by the Shapiro-Wilk normality test ($p > 0.05$), and skewness was nearly zero, indicating a symmetrical dataset. Normality cannot be assumed for air temperature values ($p < 0.05$), which ranged from 8.4 °C to 27.9 °C with a mean value of 16.6 °C. The monthly precipitation amount was better described by a log-normal distribution. The positive skewness indicates a large influence of months with a high precipitation amount, as also evidenced by the difference between the median (40 mm) and the mean value (56 mm). The amount-weighted mean $\delta^{18}O$ (and δ^2H) value was more negative than the arithmetic mean (Table 1), whereas the amount-weighted mean d-excess was higher.

The $\delta^{18}O$ (and δ^2H) values of monthly precipitation collected on Pianosa Island showed a large seasonal variability (Fig. 4, Table 2), which roughly followed the temperature and rainfall amount trends. $\delta^{18}O$ tended to be more negative during colder and rainier periods, with the lowest value in winter, and more positive during warmer and drier periods, with the highest value in summer (Table 2). Spring and autumn showed intermediate values, with lower values in autumn. The minimum $\delta^{18}O$ value was registered in January 2019, despite the rather low precipitation amount (ca. 20 mm). The maximum $\delta^{18}O$ value was instead measured in June 2021, when the temperature was high (23.2 °C) and the precipitation amount very low (ca. 2 mm). The amount-weighted seasonal mean $\delta^{18}O$ was more negative than

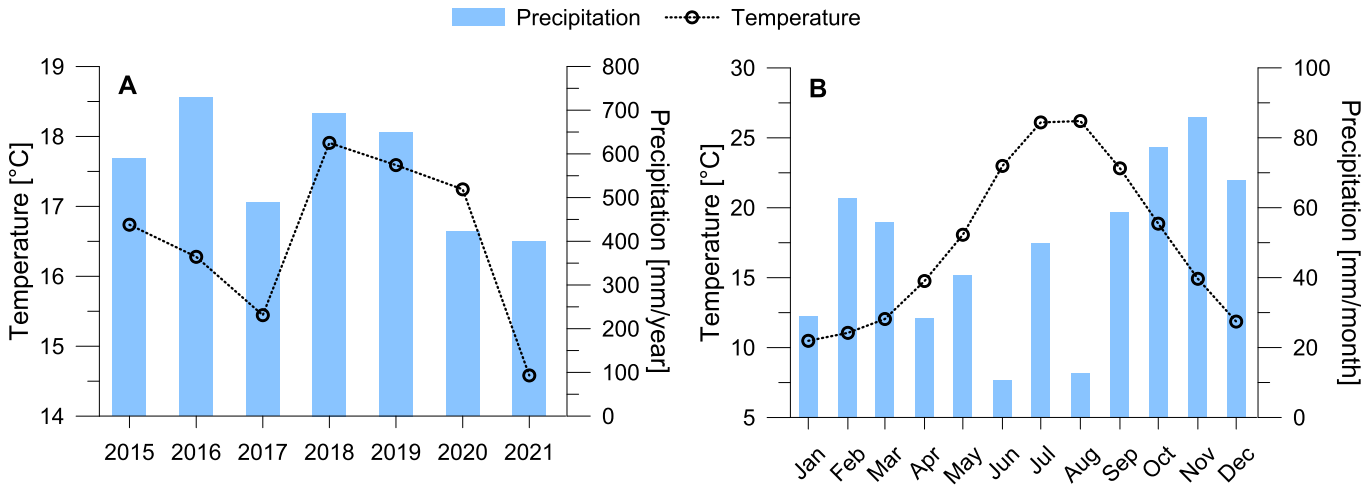

Fig. 2. A) Annual mean temperature and total annual mean precipitation on Pianosa Island; B) monthly mean temperature and monthly mean precipitation on Pianosa Island over the monitoring period (2015–2021).

Table 1
Summary statistics of isotopic parameters of monthly precipitation collected on Pianosa Island from January 2015 to December 2021, and climate-related variables.

Parameter	n	min.	1st Qu.	median	mean	$mean_w$	sd	3rd Qu.	max	Skewness	Kurtosis
Temperature (°C)	71	8.4	12.0	15.1	16.6	/	± 5.2	20.2	27.9	0.46	−0.96
Prec. amount (mm)	71	2.0	18	40	56	/	± 51	81	187	1.10	0.11
$\delta^{18}O$ ‰	71	−10.5	−7.14	−5.66	−5.36	−6.16	± 2.34	−3.52	0.6	0.11	−0.56
$\delta^{2}H$ ‰	71	−69.9	−43.4	−33.8	−31.5	−36.6	± 17.0	−17.2	9.1	0.08	−0.74
d-excess (*d*) ‰	71	2.1	8.7	11.6	11.4	12.7	± 4.4	14.5	21.7	−0.10	−0.58

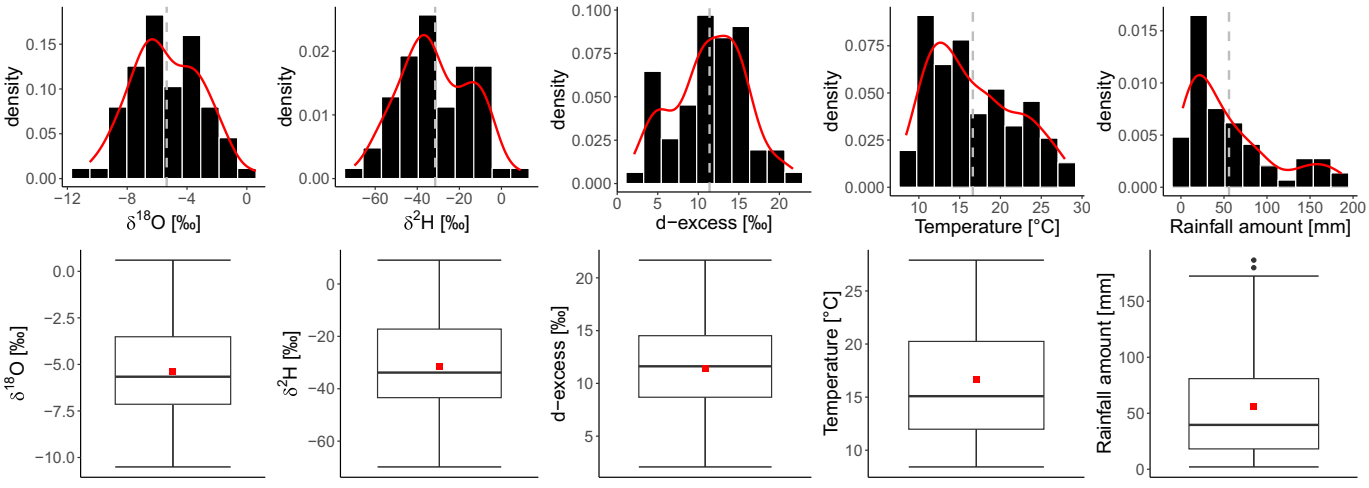

Fig. 3. Histograms (top) and boxplots (bottom) for isotopic values of monthly precipitation and climatic variables registered on Pianosa Island. The vertical dashed grey lines in the histograms indicate the mean value. The number of classes for the histograms was computed using Sturges' formula. The red square in the boxplots indicates the mean value. Lower and upper box boundaries indicate 25th and 75th percentiles, respectively, and line inside box marks the median. Whiskers above and below the box are identified with the 1.5•IQR rule; the black dots are the outliers. (For interpretation of the references to colour in this figure legend, the reader is referred to the web version of this article.)

arithmetic means, with a larger difference in summer and spring ($\Delta\delta^{18}O$ of −1.55‰ and − 0.87‰, respectively) than in winter and autumn ($\Delta\delta^{18}O$ of −0.35‰ and − 0.15‰, respectively). It is worth noting that fewer samples were collected in summer than in other seasons because this season was generally dry or characterized by very weak precipitation (Table 2).

The d-excess also seasonally changed in monthly precipitation collected on Pianosa Island (Fig. 4, Table 2). The d-excess trend roughly followed the temperature and precipitation trend and appeared anti-correlated with $\delta^{18}O$. Higher d-excess were measured in winter and autumn rains, whereas lower values were registered in spring and summer (Table 2). The lowest d-excess was registered in June 2020 (2.1‰), whereas the highest value was measured in December 2017 (21.7‰). The amount-weighted mean d-excess was higher than arithmetic means, except for autumn (Table 2). However, differences among weighted and not-weighted d-excess values were lower than the analytical error (±1.8‰), except for summer when a large difference was measured (Δd-excess of −4.4‰).

The $\delta^{18}O$, $\delta^{2}H$ and d-excess values also showed an inter-annual variability (Fig. 5, Table 3). The annual mean $\delta^{18}O$ ranged from a

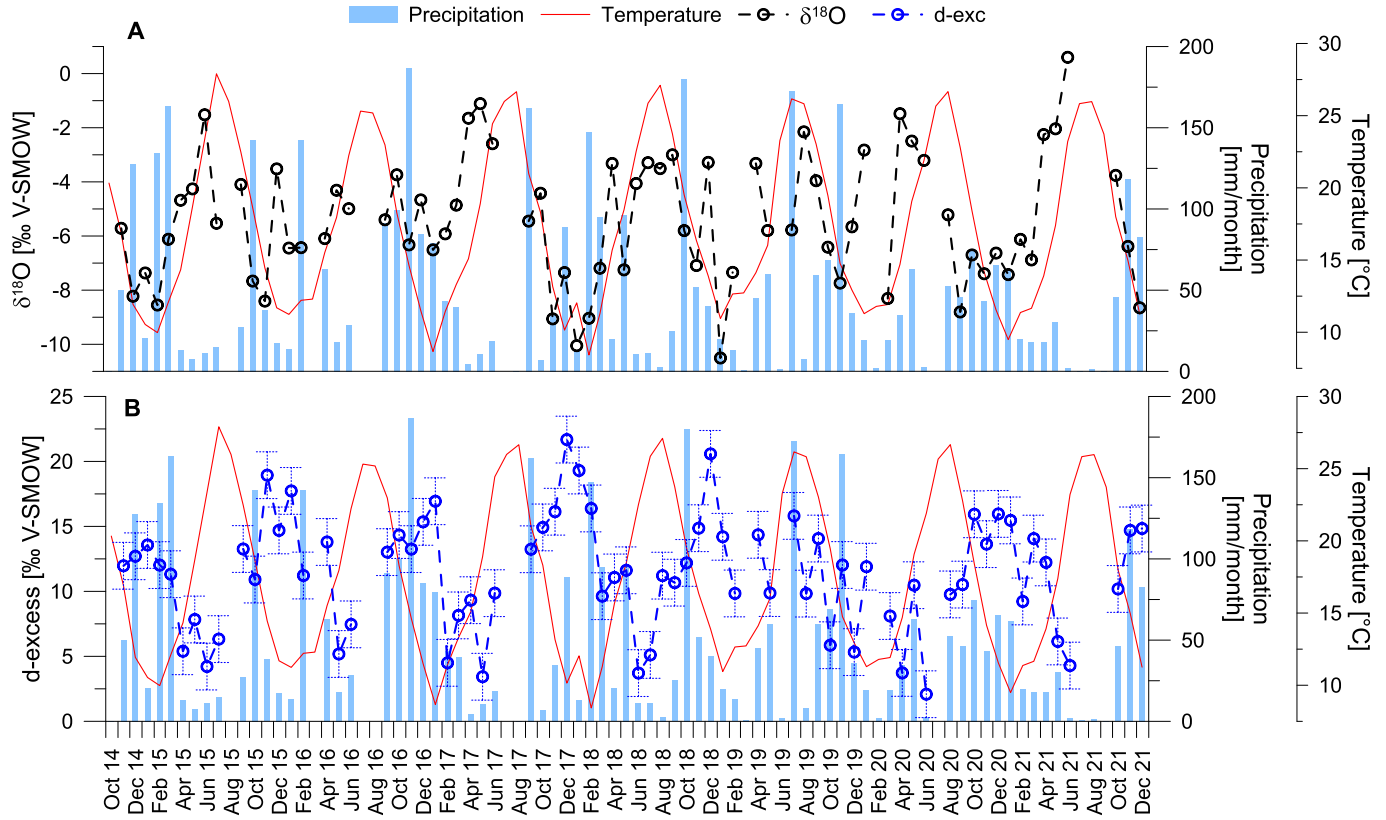

Fig. 4. Time plot of precipitation amount, atmospheric temperature, $\delta^{18}O$, and d-excess for monthly precipitation collected on Pianosa Island from October 2014 to December 2021. The error for $\delta^{18}O$ is smaller than the size of symbols; the error for d-excess is represented by the vertical bars.

Table 2
Summary statistics at seasonal scale of climate-related and isotopic variables of monthly precipitation collected on Pianosa Island from January 2015 to December 2021.

			Precipitation amount (mm)		Temperature (°C)		$\delta^{18}O$ (‰)			$\delta^{2}H$ (‰)			d-excess (‰)		
Code	Season	*n*	*mean*	*sd*	*mean*	*sd*	*mean*	*sd*	$mean_w$	*mean*	*sd*	$mean_w$	*mean*	*sd*	$mean_w$
PLP	DJF	20	164	64	11.2	1.4	−6.71	2.09	−7.06	−39.7	16.8	−42.1	14.0	4.5	14.4
	MAM	19	117	59	15.3	2.6	−4.39	2.22	−5.26	−25.9	16.7	−31.7	9.2	3.4	10.3
	JJA	12	48	61	24.8	2.1	−3.44	1.86	−4.99	−20.0	13.7	−28.0	7.5	3.9	11.9
	SON	20	238	77	18.4	3.4	−6.08	1.82	−6.23	−35.5	14.3	−37.0	13.1	2.7	12.9

minimum of −5.87‰ in 2019 to a maximum of −4.77‰ in 2021; the annual mean d-excess ranged from a minimum of 10.2‰ in 2020 to a maximum of 12.4‰ in 2016. The amount-weighted annual mean $\delta^{18}O$ was more negative than the arithmetic means, whereas the amount-weighted annual mean d-excess was higher than the arithmetic ones, even though differences were lower than the analytical error and, therefore, negligible.

4.3. Back-trajectories and moisture uptake regions of precipitating air masses

A total of 959 trajectories were obtained for monthly precipitation collected on Pianosa Island from January 2015 to December 2021 (Fig. 6a). All the trajectories calculated for each month in the period 2015–2021 are reported in Appendix B. The PFU_r and PMU_r values for each month are reported in Table A.2 and shown in boxplots of Fig. 7, whereas the mean moisture uptake over the entire period is given in Fig. 6b. The *wM_It* region was the most frequent region where the moisture uptake occurred, as indicated by the highest mean PFU_r of 48% (±17%) and ranging from a minimum of 16% in December 2019 to a maximum of 100% in July 2015, April 2017 and August 2019. The moisture uptake always occurred within the *wM_It* region during each month over the monitoring period, even if with a wide monthly variability as indicated by the large standard deviation (Fig. 7). Other important regions where the moisture uptake rather frequently occurred were the *nw* and *nA* regions, with a mean PFU_r of 15% (±12%) and 11% (±11%), respectively (Fig. 7). However, moisture was not picked (PFU_r = 0%) from these two regions in some months, whereas the maximum percentage frequency was 68% for the *nw* region in May 2015 and 39% for the *nA* in December 2019. Other areas showed mean PFU_r values lower than 10% and *pA_IP* and *nAf* regions were the most frequent, with a mean PFU_r of 9% (±11%) and 8% (±8%), respectively. The moisture uptake above the other regions rarely occurred. Although the most frequent regions where the moisture uptake occurred were also generally the regions with higher moisture fraction picked from, a slight difference may be observed between PFU_r and PMU_r values (Fig. 7). Interestingly, the PMU_r of the *wM_It* region was higher than the PFU_r, with a mean value of 59% (±17%), and ranging from a minimum of 18% in July 2017 to a maximum of 100% in the same months when the PFU_r values were maximum. On the contrary, the fraction of moisture picked from the *nw* and *nA* regions were lower than the frequency of moisture uptake above these areas (Fig. 7), as indicated by the lower PMU_r values

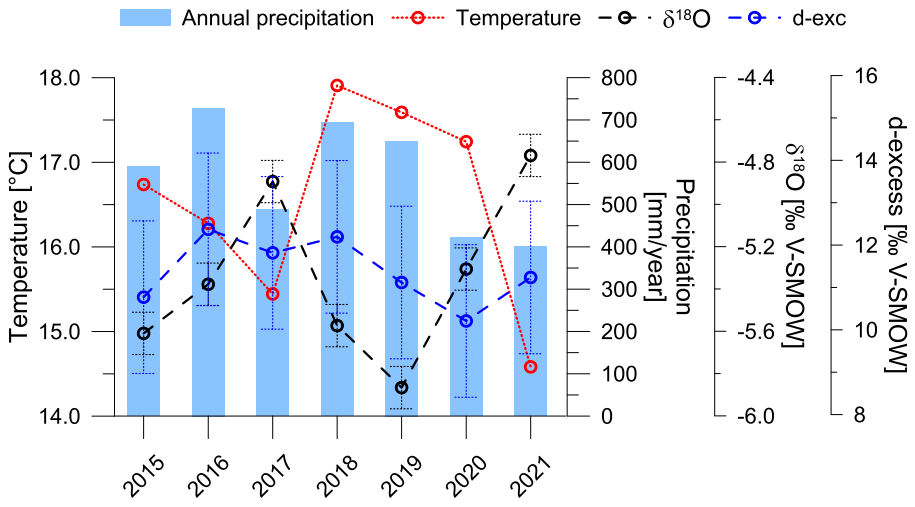

Fig. 5. Annual variability of precipitation amount, atmospheric temperature, $\delta^{18}O$ and d-excess for monthly precipitation collected on Pianosa Island from January 2015 to December 2021. The analytical errors for $\delta^{18}O$ and d-excess are represented by the vertical bars.

Table 3
Summary statistics at annual scale of climate-related and isotopic variables of monthly precipitation collected on Pianosa Island from January 2015 to December 2015.

			Precipitation amount (mm)	Temperature (°C)	$\delta^{18}O$ (‰)			$\delta^{2}H$ (‰)			d-excess (‰)		
Code	Year	*n*	*mean*	*mean*	*sd*	*mean*	*sd*	$mean_w$	*mean*	*sd*	$mean_w$	*mean*	*sd*	$mean_w$
PLP	2015	11	590	16.7	5.9	−5.61	2.24	−6.91	−34.1	15.8	−43.6	10.8	4.5	11.7
	2016	9	728	16.3	4.4	−5.38	1.01	−5.56	−30.6	7.7	−31.6	12.4	3.9	12.9
	2017	10	488	15.4	5.1	−4.89	2.53	−5.96	−27.3	17.0	−33.7	11.8	5.8	14.0
	2018	12	694	17.9	6.0	−5.57	2.50	−6.66	−32.4	18.2	−40.1	12.2	5.0	13.1
	2019	10	650	17.6	5.6	−5.87	2.39	−6.14	−35.8	19.3	−36.9	11.1	3.6	12.2
	2020	10	422	17.2	5.4	−5.31	2.63	−5.62	−32.2	19.2	−33.1	10.2	4.6	11.9
	2021	9	400	14.6	4.3	−4.77	3.06	−6.17	−26.9	21.1	−36.1	11.2	4.0	13.2

than the PFU_r ones. The mean PMU_r values were 12% (±11%) and 5% (±6%) for *nw* and *nA* regions, up to a maximum of 54% and 23%, respectively. PFU_r and PMU_r were instead very similar for *pA_IP* and *nAf* regions, whereas the moisture fraction sourced from other regions was generally very low (Fig. 7).

Slight seasonal variability in PMU_r was also observed for monthly precipitation collected on Pianosa Island over the investigated period (Fig. 8). The moisture fraction picked from the *wM_It* region was generally lower in winter (55%) and higher in spring (59%), autumn (60%) and summer (63%). Conversely, PMU_r of the *nA* region was higher in winter (11%) and lower in other seasons (4%, 4% and 2%, respectively). The moisture fraction sourced from the *nw* region was very similar in all seasons, except in summer when PMU_r was slightly higher (16% compared to 12% in spring and 11% in winter and autumn). Similar seasonal PMU_r values were also calculated for *pA_IP* and *nAf* regions, with higher and lower moisture uptake in summer, respectively, compared to other seasons.

5. Discussion

5.1. LMWL of the Pianosa Island

The isotopic variability registered in monthly precipitation samples collected on Pianosa Island was consistent with the monthly isotopic composition of precipitation registered in Tuscany (Natali et al., 2021) and the entire Italian Peninsula (Giustini et al., 2016; Longinelli and Selmo, 2003). The OLSR and RMA regressions and the corresponding precipitation-weighted regressions (PWLSR and PWRMA) were applied to derive the LMWL of Pianosa Island. The calculated values of rmSSE for different regressions (Table 4) indicated the PWLSR as the best-fitting model, whereas the RMA was the most suitable not-weighted model. The lower slope and intercept compared to the Global Meteoric Water Line (GMWL) (Fig. 9) indicated warmer and drier climatic conditions on the island, suggesting the existence of secondary evaporation processes of raindrops beneath the cloud base during precipitation (Gat, 2005; Gonfiantini, 1986). Rain droplets fall a long distance from the cloud base to the ground, thus increasing the possibility of raindrops evaporation, especially in warmer and drier months. The influence of sub-cloud processes on the weaker rains on Pianosa Island is also depicted by the difference between the amount-weighted mean $\delta^{18}O$ and d-excess and the arithmetic mean ones (Table 1). The weighted mean $\delta^{18}O$ was more negative than the arithmetic one because weaker precipitation with a more positive $\delta^{18}O$ had a lesser weight in the computation. Since evaporation of falling droplets was more likely in drier and warmer months (spring and summer) when weaker precipitation generally occurred, differences between the weighted mean $\delta^{18}O$ and the arithmetic ones were larger in spring and summer (Table 2). The same observation may be drawn looking at the d-excess mean values (Tables 1, 2). Differences among the weighted and not-weighted mean d-excess were higher than the propagated error (±1.8‰) only in summer when sub-cloud evaporation was more likely.

Interestingly, the mean $\delta^{18}O$ of monthly precipitation collected on Pianosa Island from January 2015 to December 2021 was more negative than the mean $\delta^{18}O$ as calculated at different sites placed at higher altitudes in the Apuan Alps area (Natali et al., 2022), a mountain range of northwestern Tuscany about 170 km north of the island. This finding is quite odd since the altitude effect, which was detected at the regional (Natali et al., 2021) and local scale (Natali et al., 2022), should produce more negative $\delta^{18}O$ values as the altitude increases. Therefore, the more negative $\delta^{18}O$ calculated for precipitation on Pianosa Island may be explained by the lower number of summer precipitation samples collected at this site but also almost by half the lower amount of

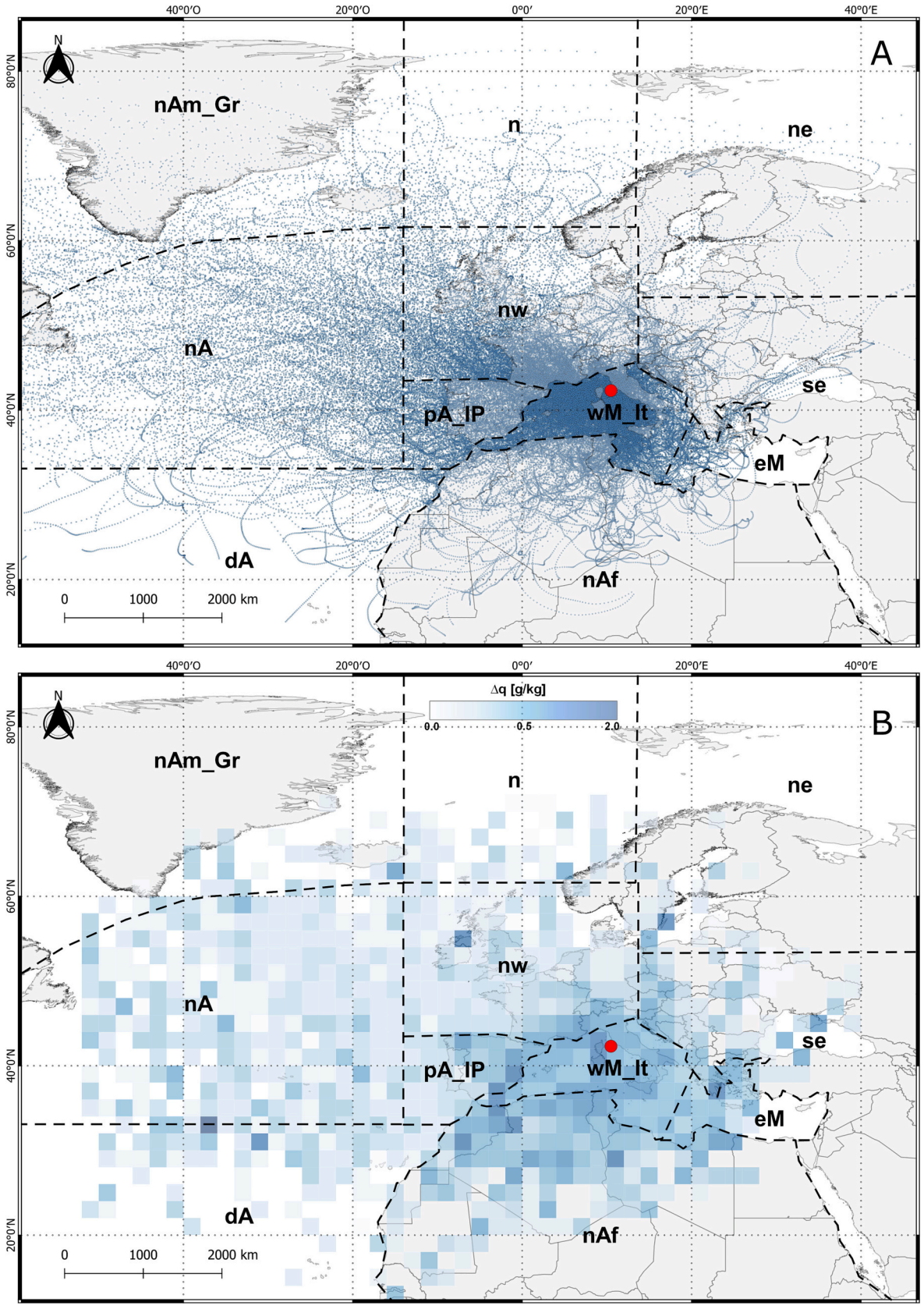

Fig. 6. A) Map of 120 h HYSPLIT backward trajectories computed for all monthly precipitation samples collected in this work. The 11 regional classes selected for classifying the events are also shown: distal Atlantic (dA); north Atlantic (nA); north America and Greenland (nAm_Gr); proximal Atlantic and Iberian Peninsula (pA_IP); north Africa (nAf); western Mediterranean and Italy (wM_It); eastern Mediterranean (eM); southeast (se); northeast (ne); north (n); northwest (nw); B) Map of moisture uptake locations in the period 2015–2021. Moisture uptake values drawn in this figure are derived by meaning the moisture fractions picked from each region during each month.

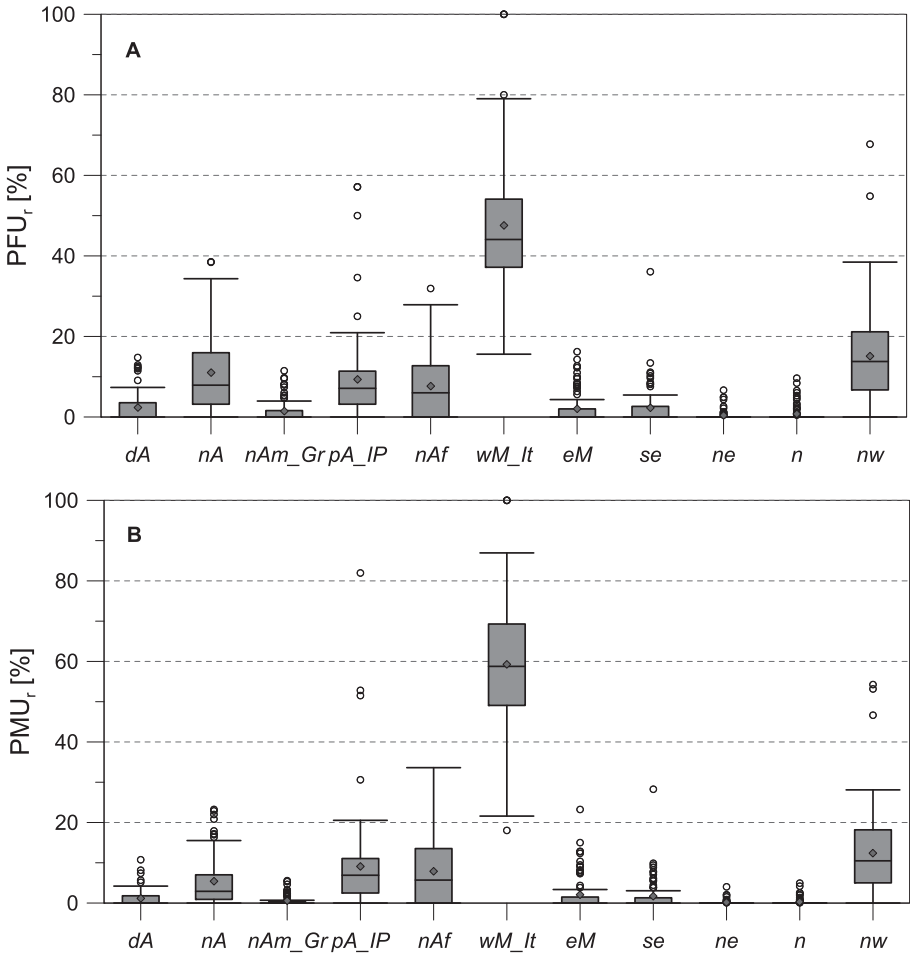

Fig. 7. Boxplot for PFU_r (Percentage Frequency of moisture Uptake for each region for each month) and PMU_r (Percentage of Moisture Uptake for each region for each month). The red square in the boxplots indicates the mean value. Lower and upper box boundaries indicate 25th and 75th percentiles, respectively, and line inside box marks the median. Whiskers above and below the box are identified with the 1.5*IQR rule; the white dots are the outliers. Classes: distal Atlantic (dA); north Atlantic (nA); north America and Greenland (nAm_Gr); proximal Atlantic and Iberian Peninsula (pA_IP); north Africa (nAf); western Mediterranean and Italy (wM_It); eastern Mediterranean (eM); southeast (se); northeast (ne); north (n); northwest (nw). (For interpretation of the references to colour in this figure legend, the reader is referred to the web version of this article.)

precipitation in this season. Precipitation was often absent in summer on the island, thus decreasing the mean $\delta^{18}O$ because of lower summer precipitation which was generally enriched in heavy isotopes relative to samples collected in other seasons (Longinelli et al., 2006).

5.2. Climatic effects on the precipitation isotopic composition

$\delta^{18}O$ (and $\delta^{2}H$) exhibited seasonal variability (Fig. 4) that roughly reflected the trend in air temperature and precipitation amount during the investigated period. A lead-lag relationship seems to be observed between the two climatic variables and isotopic values and the seasonal cycles are apparently not synchronized. Actually, this seeming lagged relationship may be attributed to the fact that summer precipitation was often absent or very weak to be sampled and analysed (e.g., summer 2016, 2017, 2020 and 2021). Consequently, the more positive $\delta^{18}O$ values were often registered before the higher temperature values and lower precipitation amounts. Conversely, when summer precipitation was relatively more intense, such as in the summer of 2018, the relationship was not lagged. Moreover, the large $\delta^{18}O$ and d-excess variability makes it quite difficult to clearly identify this possible lead-lag relationship. Therefore, congruently to conclusions derived by an isotopic study performed at the regional scale (Natali et al., 2021), as well as at the local scale in the Apuan Alps area (Natali et al., 2022), the two well-known temperature effect (Dansgaard, 1964; Rozanski et al., 1993) and amount effect (Clark and Fritz, 1997) were, almost partly, responsible of the $\delta^{18}O$ variations. To evaluate the influence of these effects on the precipitation isotope composition on Pianosa Island both at the monthly, seasonal and annual scale, a Spearman's correlation analysis was performed for data from January 2015 to December 2021 (Table 5).

A moderate positive correlation was found between the monthly mean atmospheric temperature and monthly $\delta^{18}O$ in precipitation on Pianosa Island (Table 5). The relationship was also weakly linear (Fig. 10a), with a slope of +0.21‰/°C which was very similar to that obtained at regional scale (+0.19‰/°C, Natali et al., 2021). However, theoretically, to evaluate the influence of the temperature effect on the precipitation isotopic composition, the monthly mean atmospheric temperature should be calculated by using only the temperature data of rainy days. Therefore, Spearman's correlation coefficient was also calculated between the $\delta^{18}O$ and the mean temperature of rainy days. The correlation was still moderate ($r = +0.53^{***}$), although the higher r^2 and slope (0.28, +0.26‰/°C). A moderate positive correlation was also identified between the seasonal mean atmospheric temperature and seasonal mean $\delta^{18}O$ in precipitation (Table 5, Fig. 10b), and the relationship was more linear with a slope of +0.21‰/°C. Conversely, an opposite-sign correlation, although not significant, was found between $\delta^{18}O$ and annual temperature ($r = -0.75^{ns}$), with more positive $\delta^{18}O$ values as temperature increased. This result is in disagreement with the theoretical definition of the temperature effect, but more years should be used to obtain a reliable and significant relationship. A moderate negative correlation was found between the monthly total precipitation amount and monthly $\delta^{18}O$ (Table 5), which was very similar to that found at the regional scale (Natali et al., 2021). The linear relationship was weak (Fig. 10a), with a linear gradient of −1.8‰ per 100 mm/month, which was higher than that found at the regional scale (−0.8‰ per 100 mm/month, Natali et al., 2021). This correlation was stronger when applied to the seasonal total precipitation amount and seasonal mean $\delta^{18}O$, and also at the annual scale, although not significant in this latter case (Table 5). The relationship $\delta^{18}O$ vs. precipitation amount was

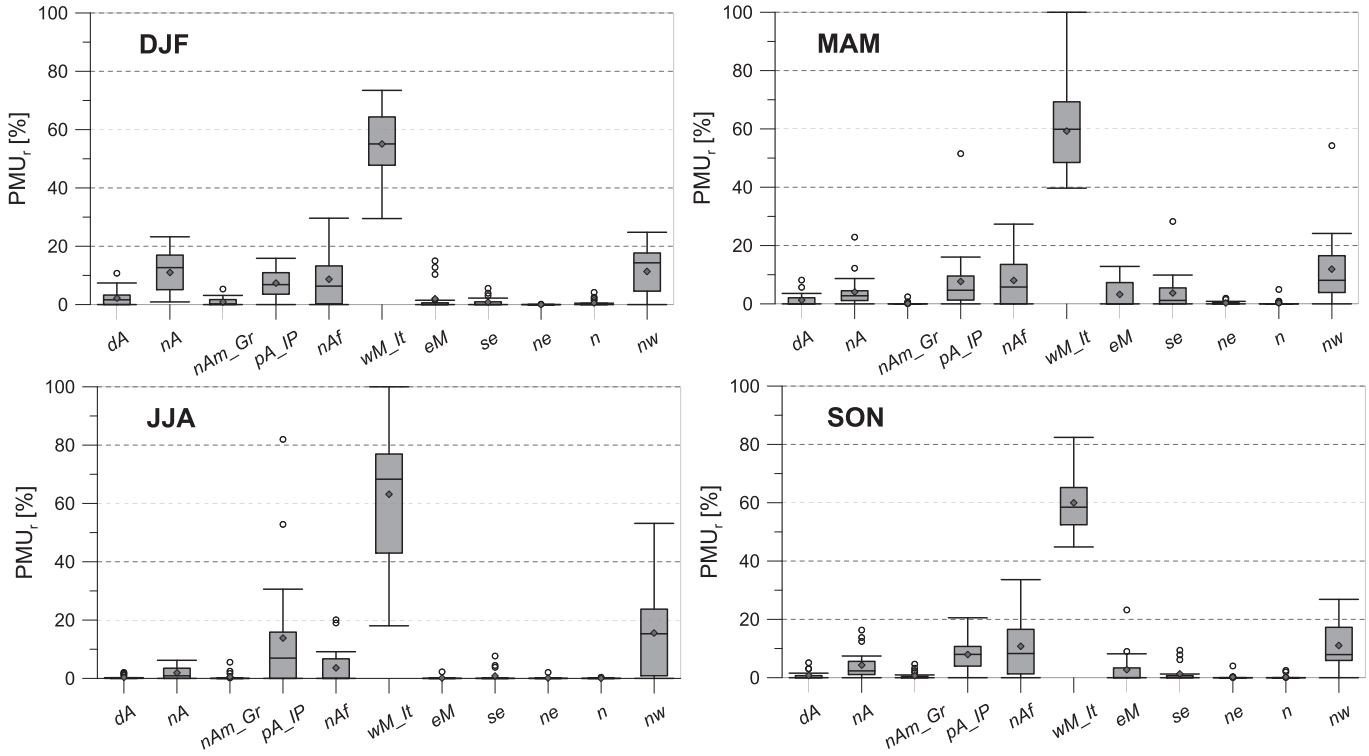

Fig. 8. Monthly variability of PMU_r of each regional class for each season. The symbols of boxplot are described in the caption of Fig. 7. Classes: distal Atlantic (dA); north Atlantic (nA); north America and Greenland (nAm_Gr); proximal Atlantic and Iberian Peninsula (pA_IP); north Africa (nAf); western Mediterranean and Italy (wM_It); eastern Mediterranean (eM); southeast (se); northeast (ne); north (n); northwest (nw).

Table 4
Monthly LMWLs computed by different regression techniques on Pianosa Island. s.e.: standard error; CI: Confidence Interval.

	n data	slope	intercept	95% CI slope		95% CI intercept		r^2	rmSSE
PLP		*value* ± *s.e.*	*value* ± *s.e.*	Upper	Lower	Upper	Lower		
OLSR	71	7.06 ± 0.20	6.36 ± 1.17	7.45	6.67	8.64	4.07	0.95	1.011
RMA	**71**	**7.25 ± 0.20**	**7.39 ± 1.15**	**7.64**	**6.87**	**9.64**	**5.13**	**0.95**	**1.004**
PWLSR	**71**	**7.39 ± 0.22**	**8.93 ± 1.44**	**7.83**	**6.95**	**11.8**	**6.12**	**0.95**	**1.000**
PWRMA	71	7.62 ± 0.23	10.4 ± 1.45	8.06	7.18	13.2	7.52	0.95	1.028

also more linear at the seasonal scale (Fig. 10b), with a gradient of −1.1‰ per 100 mm/season. Overall, congruently to the regional framework (Natali et al., 2021), temperature and amount effects contribute to explaining the 20% and 15%, respectively, of the isotopic variability observed at the monthly scale, whereas their effect is more evident at the seasonal scale.

A moderate negative correlation was found between monthly d-excess and monthly mean air temperature, as well as at the seasonal scale (Table 5, Fig. 10). This negative relationship, which was more linear when the seasonal mean temperature and d-excess were considered, proves once again the influence of sub-cloud processes on precipitation occurring on the island in warmer seasons. The correlation was instead absent at the annual scale (Table 5), probably due to the few years that were considered in this work. On the other side, a moderate-to-strong positive correlation was found between the d-excess and precipitation amount respectively at the monthly and seasonal scale (Table 5, Fig. 10), which implies decreasing d-excess values as rain amount decreases, congruently to a sub-cloud evaporation model. The relationship was much more linear when the seasonal mean d-excess and total seasonal precipitation amount were considered (Fig. 10b), whereas no significant correlation was found at the annual scale (Table 5). Overall, the d-excess seasonal variability registered on Pianosa Island from October 2014 to December 2021 was partly controlled by changes in SST and RH at the moisture sources (Bonne et al., 2019; Pfahl and Sodemann, 2014; Uemura et al., 2008), but also by the local climatic variables, whose effect overlaps and potentially obscures the original d-excess signature imprinted at the moisture source, as also indicated by very recent studies (Natali et al., 2022; Xia and Winnick, 2021; Xiang et al., 2022).

5.3. Moisture origin and "source" effect on the precipitation isotope composition

The quantitative diagnostic for moisture uptake locations applied in this work indicated the region between the western Mediterranean basin, Italy and the Adriatic Sea as the most frequent moisture source region associated with monthly precipitation samples (Fig. 7a). Moisture contributions from this area were always present in each month in the period 2015–2021, as expected since the position of the Pianosa Island approximately in the centre of the considered area. Regardless of the origin of air masses producing rainfall, all of them had to cross at least a part of this region before reaching the sampling site, where the moisture uptake occurred although with variable frequency and intensity. Moisture was less frequently picked from the northwestern areas of Europe (central-western France and the area lying between the Bay of Biscay and the North Sea), the North Atlantic Ocean, the proximal Atlantic Ocean, the Iberian Peninsula and North Africa (Fig. 7a). However, when the moisture fraction picked from each region was considered, the

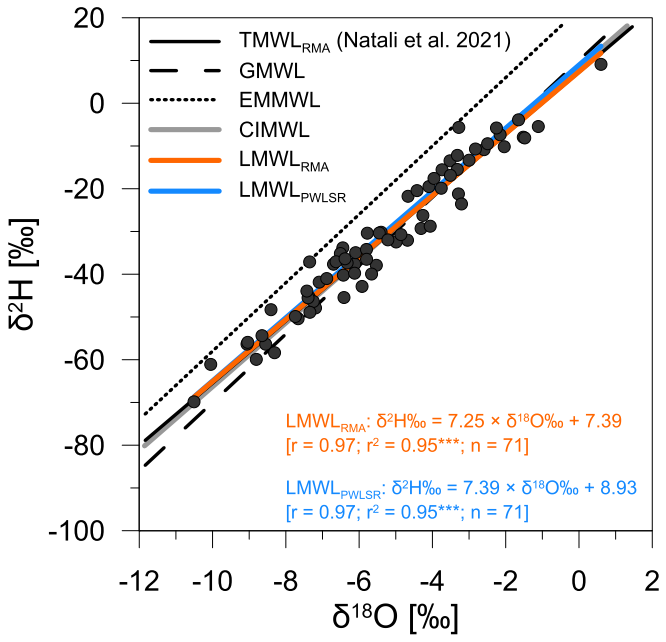

Fig. 9. δ^2H vs. $\delta^{18}O$ diagram of monthly precipitation collected at PLP (Pianosa Island). Also shown: Eastern Mediterranean Meteoric Water Line (EMMWL, Gat and Carmi, 1970); Global Meteoric Water Line (GMWL, Craig, 1961, Rozanski et al., 1993); Central Italy Meteoric Water Line (CIMWL, Giustini et al., 2016); Tuscany Meteoric Water Line (TMWL$_{RMA}$ (2), Natali et al., 2021).

Table 5
Spearman's rank correlation coefficients between $\delta^{18}O$ and d-excess and climatic variables (air temperature and precipitation amounts) at monthly, seasonal, and annual scale. ***: p-values < 0.001; **: p-values < 0.01; *: p-values < 0.05; ns: p-values higher than 0.05.

	Temperature (°C)	Precipitation (mm)
$\delta^{18}O$ (‰)		
Monthly	$+0.52^{***}$	-0.46^{***}
Seasonal	$+0.57^{**}$	-0.63^{***}
Annual	-0.75^{ns}	-0.64^{ns}
d-excess (‰)		
Monthly	-0.43^{***}	$+0.42^{***}$
Seasonal	-0.55^{**}	$+0.71^{***}$
Annual	-0.14^{ns}	$+0.60^{ns}$

moisture contribution of the western Mediterranean region to the precipitation on Pianosa Island was even higher, whereas the northwestern areas of Europe and the North Atlantic Ocean supply less humidity in relation to the frequency of moisture uptake above these regions (Fig. 7b). The moisture fraction sourced from the proximal Atlantic, the Iberian Peninsula and North Africa was also larger than the fraction picked from the North Atlantic Ocean. This outcome was consistent with the mean climatology of the study area, and a conceptual model of moisture associated with precipitation on Pianosa Island may be hypothesized. Local atmospheric disturbances, which more frequently occurred in spring, summer, and autumn (Fig. 8), mostly originated above the western Mediterranean basin and they picked the most humidity above this region, in addition to Italy and the Adriatic Sea for air masses coming from eastern sectors and to the Iberian Peninsula and North Africa for air masses coming from western and southern sectors. On the other side, more distal atmospheric disturbances, generally coming from the North Atlantic Ocean and the northwestern areas of Europe in winter, supplied much less humidity compared to more proximal regions. Air masses frequently reached the western Mediterranean with a low moisture content, probably due to prior precipitation along trajectories (i.e., rainout), thus loading humidity above more proximal regions, especially above the Mediterranean basin. This process was likely due to strong evaporation above the Mediterranean Sea, which was boosted by the relatively high sea surface temperature (SST) and by the large thermal gradient between the sea surface and atmosphere, especially in autumn (Pastor et al., 2018). However, vapour from evapotranspiration above the continental surfaces crossed by air masses also likely contributed to precipitation on Pianosa Island. It is worth noting that when quantifying the total contributions as defined in this work (PFU$_r$ and PMU$_r$) precipitation along the trajectories should be discounted because it would decrease the contribution by previous moisture uptake regions. Without considering in-route precipitation, the calculated results may overestimate distal contribution but underestimate proximal contribution. As a consequence, the moisture contribution of the more proximal regions, such as the western Mediterranean region, to precipitation on Pianosa Island would be even higher compared to a minor role of the more distal moisture source regions. This evidence confirms the primary role of the western Mediterranean in supplying moisture to precipitation above the study area.

In order to evaluate the influence of moisture origin on the isotopic composition of precipitation on Pianosa Island, Spearman's correlation analysis was applied between the climatic variables (temperature and precipitation amount), $\delta^{18}O$ and d-excess and PMU$_r$ of each region (Table 6). Interestingly, among the most frequent regions, the PMU$_r$ of *wM_It* and *nAf* regions showed a weak positive and significant correlation with $\delta^{18}O$, although the significance for *nAf* was lower and within the 90% confidence level. On the contrary, the PMU$_r$ of *nw* and *nA* regions exhibited a weak-to-moderate negative and significant correlation with $\delta^{18}O$, with the significance for *nw* at a 90% confidence level. The PMU$_r$ of *nA* was also negatively correlated with the atmospheric temperature, whereas the PMU$_r$ of *nw* was positively correlated. No significant correlations were found between the PMU$_r$ and $\delta^{18}O$ for other regions. These results indicated that the higher the moisture fraction picked from the western Mediterranean basin, Italy, the Adriatic Sea, and North Africa, the more positive the $\delta^{18}O$ of precipitation occurring on Pianosa Island. On the other side, the higher the percentage of moisture sourced from the North Atlantic Ocean and northwestern regions of Europe (France, Bay of Biscay, North Sea), the more negative the $\delta^{18}O$. These patterns are consistent with the rainout effect (Dansgaard, 1964) since Pianosa Island is located in the western Mediterranean (Tyrrhenian Sea) and moisture picked from this basin and more proximal regions is carried by air masses over a much shorter distance compared to humidity coming from more distal areas (e.g., the North Atlantic Ocean). Moreover, the Mediterranean Sea tends to be isotopically enriched in heavy isotopes compared to the Atlantic Ocean (LeGrande and Schmidt, 2006) and SST and atmospheric conditions above the evaporating surface may also produce different isotope signatures in evaporative flows. On the other side, precipitating air masses supplied by moisture picked from more distal regions, such as the North Atlantic Ocean and northwestern regions of Europe, were characterized by a longer rainout distance, thus producing more negative $\delta^{18}O$ values. Interestingly, the moisture fraction picked from the North Atlantic Ocean was higher when the temperature was lower on the island, suggesting a prevalence of this condition in winter that is congruent with the NAO-linked origin of atmospheric disturbances in the Mediterranean area during this season (López-Moreno et al., 2011; Luppichini et al., 2022; Luppichini et al., 2021).

Concerning the d-excess, no significant correlations were found with PMU$_r$ (Table 6), except for a very weak negative correlation for the *pA_IP* region and significant at a 90% confidence level. This outcome indicated that d-excess should not be used to distinguish Mediterranean precipitation from Atlantic ones (Natali et al., 2022), because no significant difference may be identified among these two source areas. Interpreting high d-excess values in precipitation as the result of more intense evaporation above the Mediterranean Sea, which leads to more intense moisture uptake, may be erroneous and imprecise. The lack of correlation between the d-excess and PMU$_r$ could be due to secondary

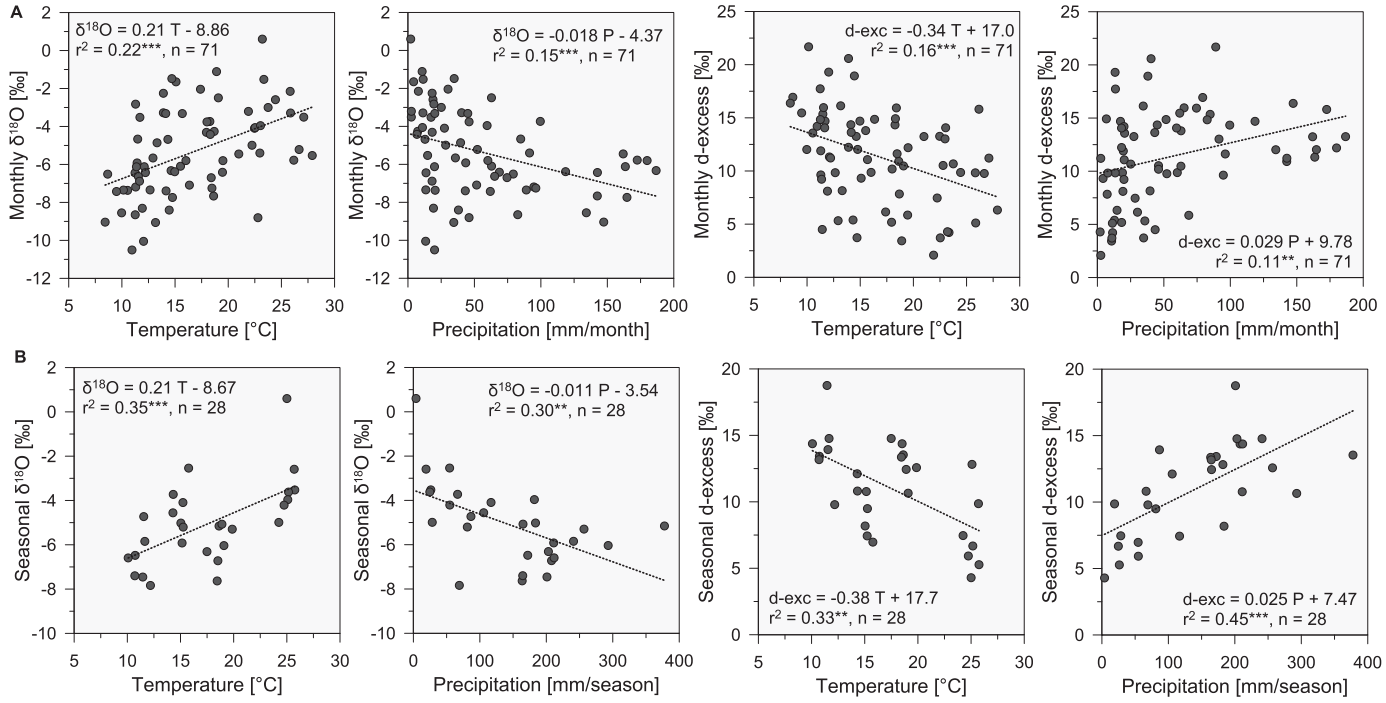

Fig. 10. Correlation plots between $\delta^{18}O$ and d-excess of monthly precipitation collected on Pianosa Island and climatic variables (atmospheric temperature and precipitation amount) at A) monthly scale ($n = 71$) and B) seasonal scale ($n = 28$).

Table 6
Spearman's correlations coefficients between the PMU_r of each region and climatic and isotopic variables. ***: p-values < 0.001; **: p-values < 0.01; *: p-values < 0.05; ns: p-values higher than 0.10. Significant correlations are in bold.

Regions (r)	*mean* PMUr [%]	Temperature (°C)	Precipitation (mm)	$\delta^{18}O$ (‰)	d-excess (‰)
dA	1	-0.18^{ns}	$+0.05^{ns}$	-0.14^{ns}	-0.22^{ns}
nA	5	**-0.44*****	$+0.15^{ns}$	**-0.40****	$+0.19^{ns}$
nAm_Gr	1	-0.18^{ns}	$+0.01^{ns}$	-0.20^{ns}	$+0.06^{ns}$
pA_IP	9	$+0.15^{ns}$	$+0.02^{ns}$	$+0.08^{ns}$	**-0.22**
nAf	8	-0.05^{ns}	$+0.01^{ns}$	**$+0.22$**	$+0.02^{ns}$
wM_It	59	$+0.16^{ns}$	-0.13^{ns}	**$+0.27$***	-0.11^{ns}
eM	2	$+0.03^{ns}$	-0.18^{ns}	$+0.26^{ns}$	$+0.10^{ns}$
se	2	$+0.19^{ns}$	-0.05^{ns}	$+0.10^{ns}$	-0.22^{ns}
ne	<1	$+0.42^{ns}$	**-0.42***	$+0.26^{ns}$	-0.29^{ns}
n	<1	-0.23^{ns}	-0.18^{ns}	-0.20^{ns}	$+0.11^{ns}$
nw	12	**$+0.22$**	-0.13^{ns}	**-0.21**	$+0.10^{ns}$

evaporative processes (i.e. sub-cloud evaporation) and/or other processes occurring during the humidity transport able to modify the d-excess values imprinted at the moisture uptake source (Natali et al., 2022; Xiang et al., 2022), cancelling any relationships with the source region.

5.4. A linear model for predicting the $\delta^{18}O$ in precipitation by temperature, precipitation amount and moisture origin

In the previous sections, the influence of temperature, amount and source effects on the $\delta^{18}O$ of precipitation on Pianosa Island has been evaluated separately by applying Spearman's correlation analysis and simple linear regression models. As all these effects emerged as controls on the precipitation isotope composition, although with different intensities, we applied a multiple linear regression model for predicting $\delta^{18}O$ values in precipitation. In order to define the I_{MED}, which is an index of the Mediterranean character of each monthly precipitation sample, only regions with a higher mean PMU_r and having a significant correlation with the $\delta^{18}O$ (Table 6) were considered: the *wM_It* and *nAf* regions, for positive correlations between PMU_r and $\delta^{18}O$; the *nA* and *nw* regions, for negative correlations. The index was therefore defined for each monthly precipitation sample as follows:

$$I_{MED} = \frac{PMU_{wM\_It} + PMU_{nAf}}{PMU_{wM\_It} + PMU_{nAf} + PMU_{nA} + PMU_{nw}} \bullet 100$$

where I_{MED} provides an estimate of the Mediterranean character of precipitation as expressed by the ratio between the sum of moisture fraction (i.e., PMU_r) picked from more proximal regions around the precipitation collection site (*wM_It* and *nAf* regions) and the total moisture fraction source from all the four regions. The higher the I_{MED} value, the larger the moisture fraction picked from proximal regions (i.e., Mediterranean areas). Therefore, a multivariate linear model was created for predicting $\delta^{18}O$ values in precipitation by using the monthly mean temperature (T), the total monthly precipitation amount (P) and the I_{MED}: $\delta^{18}O = 0.16\ T - 0.01P + 0.05I_{MED} - 10.4$ ($r^2 = 0.47$***, r^2 adjusted = 0.45***). This model explains 45% of the $\delta^{18}O$ variability. The regression β coefficients express the change in the dependent variable $\delta^{18}O$ following a unitary change in one of the regressors, provided that the value of the other regressors remains constant. However, the values of the coefficients depend on the unit of measurement of the variable to which they are associated, therefore they cannot be directly compared and used to establish an order of importance among the regressors with respect to the impact on the dependent variable. For this purpose, the standardized regression β coefficients are useful for evaluating the relative importance of regressors, as they are not influenced by the unit of measurement of the variables. The regressors T and I_{MED} had a higher coefficient (+0.39 and + 0.36, respectively) compared to the variable P (−0.28), indicating the source and temperature effects as the main effects affecting the $\delta^{18}O$ in precipitation, compared to the amount effect.

6. Conclusions

In this work, we presented and discussed the results of multi-year

isotopic monitoring in the period 2014–2021 of monthly precipitation collected on Pianosa Island (Italy), a small island located in the northern Tyrrhenian Sea (western Mediterranean). The LMWL of this Mediterranean island was defined for the first time by using different regression techniques. The lower slope and intercept compared to the GMWL indicated warmer and drier climatic conditions on the island, suggesting the existence of sub-cloud evaporation processes of raindrops during precipitation, especially in summer. The lack of precipitation in summer, when higher $\delta^{18}O$ values were generally registered, was likely responsible for the more negative mean $\delta^{18}O$ of monthly precipitation collected on Pianosa Island. The influence of temperature, amount, and source effects on the $\delta^{18}O$ of precipitation was evaluated firstly separately by applying Spearman's correlation analysis and simple linear regression models; then, a multiple linear regression model was applied for predicting $\delta^{18}O$ values in precipitation. When taken apart, temperature and amount effects contribute to explain the 20% and 15%, respectively, of the $\delta^{18}O$ variability observed at the monthly scale, whereas their effect is more evident at the seasonal scale. The HYSPLIT-based moisture uptake analysis performed in this work indicated the effect of moisture origin and rainout on the isotope composition of precipitation. The region between the western Mediterranean basin, Italy, and the Adriatic Sea was the most frequent moisture source region and supplied most of the humidity associated with monthly precipitation samples on Pianosa Island. Less moisture was picked from the northwestern areas of Europe, such as central-western France and the area lying between the Bay of Biscay and the North Sea, the North Atlantic Ocean, the proximal Atlantic Ocean, the Iberian Peninsula and North Africa. Results from this study indicated that consistently with the rainout effect, the higher the moisture fraction picked from the more proximal regions (such as the western Mediterranean basin, Italy, the Adriatic Sea, and North Africa), the more positive the $\delta^{18}O$ of precipitation occurring on Pianosa Island; conversely, the higher the percentage of moisture sourced from more distal regions (such as the North Atlantic Ocean and northwestern regions of Europe), the more negative the $\delta^{18}O$. The model resulting from the multivariate regression indicated that 45% of the $\delta^{18}O$ variability may be explained by temperature, amount and source effects. However, among these effects, moisture origin and temperature were major controls on the $\delta^{18}O$ in precipitation, compared to the precipitation amount.

Overall, the d-excess seasonal variability registered on Pianosa Island from October 2014 to December 2021 was partly controlled by changes in SST and RH at the moisture sources, but also by the local climatic variables such as temperature and precipitation amount, whose effect overlaps and potentially obscures the original d-excess signature imprinted at the moisture source. No correlation was found between the precipitation d-excess and the moisture fraction picked from any regions, suggesting that the d-excess should not be used to distinguish precipitation coming from the Mediterranean basin from those originating in the North Atlantic Ocean, because no significant difference may be identified among these two source areas. Interpreting high d-excess values in precipitation as the result of more intense evaporation above the Mediterranean Sea, which leads to more intense moisture uptake, may be erroneous. Sub-cloud evaporation may represent one of the reasons why the d-excess did not show any relationships with moisture source regions, along with other processes occurring during the humidity transport able to modify the d-excess values imprinted at the moisture uptake source, cancelling any relationships with the source region. This suggested that more caution should be paid when using the d-excess as a tracer of moisture origin and climatic conditions at the evaporative areas.

CRediT authorship contribution statement

Stefano Natali: Conceptualization, Methodology, Software, Validation, Formal analysis, Investigation, Data curation, Writing – original draft, Writing – review & editing, Visualization. **Marco Doveri:** Investigation, Resources, Data curation, Writing – review & editing, Project administration, Funding acquisition. **Linda Franceschi:** Investigation, Data curation, Writing – review & editing. **Roberto Giannecchini:** Investigation, Resources, Writing – review & editing, Project administration, Funding acquisition. **Marco Luppichini:** Software, Formal analysis, Writing – review & editing. **Matia Menichini:** Investigation, Data curation, Writing – review & editing. **Giovanni Zanchetta:** Writing – review & editing, Supervision.

Declaration of Competing Interest

The authors declare that they have no known competing financial interests or personal relationships that could have appeared to influence the work reported in this paper.

Data availability

All the data are available in the supplementary materials

Acknowledgements

This work is part of the PhD project of Stefano Natali. The authors would thank the primary funders of this research: the Province of Livorno (Prot. IGG/CNR 1448/2015); the Tuscan Archipelago National Park (Prot. IGG/CNR 221/2018); the funding international program of UNESCO and the abrdn Charitable Foundation - Promoting sustainable development through UNESCO's programmes and sites - which funded the project Hydro-Island (Pianosa Island: hydrological processes and water resources sustainability in a climate-changing Mediterranean) (Prot. IGG/CNR 224994/2023). The authors also thank the penitentiary police of the island for its support during monitoring.

Appendix A. Supplementary data

Supplementary data to this article can be found online at https://doi.org/10.1016/j.atmosres.2023.106987.

References

Alpert, P., Ben-Gai, T., Baharad, A., Benjamini, Y., Yekutieli, D., Colacino, M., Diodato, L., Ramis, C., Homar, V., Romero, R., Michaelides, S., Manes, A., 2002. The paradoxical increase of Mediterranean extreme daily rainfall in spite of decrease in total values. Geophys. Res. Lett. 29, 31–34. https://doi.org/10.1029/2001GL013554.

Amin, A., Zuecco, G., Geris, J., Schwendenmann, L., McDonnell, J.J., Borga, M., Penna, D., 2020. Depth distribution of soil water sourced by plants at the global scale: a new direct inference approach. Ecohydrology 13, e2177. https://doi.org/10.1002/eco.2177.

Baldini, L.M., McDermott, F., Foley, A.M., Baldini, J.U.L., 2008. Spatial variability in the European winter precipitation δ18O-NAO relationship: implications for reconstructing NAO-mode climate variability in the Holocene. Geophys. Res. Lett. 35 https://doi.org/10.1029/2007GL032027.

Baldini, L.M., McDermott, F., Baldini, J.U.L., Fischer, M.J., Möllhoff, M., 2010. An investigation of the controls on Irish precipitation δ18O values on monthly and event timescales. Clim. Dyn. 35, 977–993. https://doi.org/10.1007/s00382-010-0774-6.

Bates, B.C., Kundzewicz, Z.W., Wu, S., Palutikof, J.P., 2008. Climate change and water. In: Technical Paper of the Intergovernmental Panel on Climate Change. IPCC Secretariat, Geneva.

Bershaw, J., Penny, S.M., Garzione, C.N., 2012. Stable isotopes of modern water across the Himalaya and eastern Tibetan Plateau: Implications for estimates of paleoelevation and paleoclimate. J. Geophys. Res. Atmos. 117 https://doi.org/10.1029/2011JD016132.

Blöschl, G., Hall, J., Viglione, A., Perdigão, R.A.P., Parajka, J., Merz, B., Lun, D., Arheimer, B., Aronica, G.T., Bilibashi, A., Boháč, M., Bonacci, O., Borga, M., Čanjevac, I., Castellarin, A., Chirico, G.B., Claps, P., Frolova, N., Ganora, D., Gorbachova, L., Gül, A., Hannaford, J., Harrigan, S., Kireeva, M., Kiss, A., Kjeldsen, T.R., Kohnová, S., Koskela, J.J., Ledvinka, O., Macdonald, N., Mavrova-Guirguinova, M., Mediero, L., Merz, R., Molnar, P., Montanari, A., Murphy, C., Osuch, M., Ovcharuk, V., Radevski, I., Salinas, J.L., Sauquet, E., Šraj, M., Szolgay, J., Volpi, E., Wilson, D., Zaimi, K., Živković, N., 2019. Changing climate both increases and decreases European river floods. Nature 573, 108–111. https://doi.org/10.1038/s41586-019-1495-6.

Bonne, J.-L., Behrens, M., Meyer, H., Kipfstuhl, S., Rabe, B., Schönicke, L., Steen-Larsen, H.C., Werner, M., 2019. Resolving the controls of water vapour isotopes in

the Atlantic sector. Nat. Commun. 10, 1632. https://doi.org/10.1038/s41467-019-09242-6.
Bowen, G.J., Cai, Z., Fiorella, R.P., Putman, A.L., 2019. Isotopes in the water cycle: regional- to global-scale patterns and applications. Annu. Rev. Earth Planet. Sci. 47, 453–479. https://doi.org/10.1146/annurev-earth-053018-060220.
Brunet, M., SaladiÉ, O., Jones, P., SigrÓ, J., Aguilar, E., Moberg, A., Lister, D., Walther, A., Lopez, D., Almarza, C., 2006. The development of a new dataset of Spanish Daily Adjusted Temperature Series (SDATS) (1850–2003). Int. J. Climatol. 26, 1777–1802. https://doi.org/10.1002/joc.1338.
Brunetti, M., Maugeri, M., Monti, F., Nanni, T., 2006. Temperature and precipitation variability in Italy in the last two centuries from homogenised instrumental time series. Int. J. Climatol. 26, 345–381. https://doi.org/10.1002/joc.1251.
Caloiero, T., Coscarelli, R., Ferrari, E., Mancini, M., 2011. Precipitation change in Southern Italy linked to global scale oscillation indexes. Nat. Hazards Earth Syst. Sci. 11, 1683–1694. https://doi.org/10.5194/nhess-11-1683-2011.
Casellas, E., Latron, J., Cayuela, C., Bech, J., Udina, M., Sola, Y., Lee, K.-O., Llorens, P., 2019. Moisture origin and characteristics of the isotopic signature of rainfall in a Mediterranean mountain catchment (Vallcebre, eastern Pyrenees). J. Hydrol. 575, 767–779. https://doi.org/10.1016/j.jhydrol.2019.05.060.
Chan, D., Wu, Q., 2015. Significant anthropogenic-induced changes of climate classes since 1950. Sci. Rep. 5, 13487. https://doi.org/10.1038/srep13487.
Clark, I., Fritz, P., 1997. Environmental Isotopes in Hydrogeology. CRC Press/Lewis Publishers, Boca Raton.
Comas-Bru, L., McDermott, F., Werner, M., 2016. The effect of the East Atlantic pattern on the precipitation δ18O-NAO relationship in Europe. Clim. Dyn. 47, 2059–2069. https://doi.org/10.1007/s00382-015-2950-1.
Coppola, E., Giorgi, F., 2010. An assessment of temperature and precipitation change projections over Italy from recent global and regional climate model simulations. Int. J. Climatol. 30, 11–32. https://doi.org/10.1002/joc.1867.
Crawford, J., Hughes, C.E., Lykoudis, S., 2014. Alternative least squares methods for determining the meteoric water line, demonstrated using GNIP data. J. Hydrol. 519, 2331–2340. https://doi.org/10.1016/j.jhydrol.2014.10.033.
Cruz-San, J., Araguas, L., Rozanski, K., Benavente, J., Cardenal, J., Hidalgo, M.C., Garcia-Lopez, S., Martinez-Garrido, J.C., Moral, F., Olias, M., 1992. Sources of precipitation over South-Eastern Spain and groundwater recharge. An isotopic study. Tellus B 44, 226–236. https://doi.org/10.1034/j.1600-0889.1992.t01-2-00005.x.
Dansgaard, W., 1964. Stable isotopes in precipitation. Tellus 16, 436–468. https://doi.org/10.1111/j.2153-3490.1964.tb00181.x.
Doveri, M., Giannecchini, R., Mussi, M., Nicotra, I., Puccinelli, A., 2012. Aspetti geologici e idrogeologici del peculiare acquifero dell'Isola di Pianosa (Arcipelago Toscano). Ital. J. Eng. Geol. Environ. 15, 17–30. https://doi.org/10.1474/EHEGeology.2012-15.0-0.2.0292.
Doveri, M., Stenni, B., Petrini, R., Giannecchini, R., Dreossi, G., Menichini, M., Ghezzi, L., 2019. Oxygen and hydrogen isotopic composition of waters in a past-mining area of southern Apuan Alps (Italy): hydrogeological characterization and implications on the fate of potentially toxic elements. J. Geochem. Explor. https://doi.org/10.1016/j.gexplo.2019.106338.
Dumitru, O.A., Forray, F.L., Fornós, J.J., Ersek, V., Onac, B.P., 2017. Water isotopic variability in Mallorca: a path to understanding past changes in hydroclimate. Hydrol. Process. 31, 104–116. https://doi.org/10.1002/hyp.10978.
Epstein, S., Mayeda, T., 1953. Variation of O^{18} content of waters from natural sources. Geochim. Cosmochim. Acta 4, 213–224. https://doi.org/10.1016/0016-7037(53)90051-9.
European Environment Agency, 2019. Economic Losses from Climate -Related Extremes in Europe. Indicator Assessment.
Fletcher, T., 2022. QuantPsyc: Quantitative Psychology Tools. https://CRAN.R-project.org/package=QuantPsyc.
Foresi, L., Cornamusini, G., Bossio, A., Mazzei, R., Salvatorini, G., Argenti, P., 2000. La successione miocenica dell'Isola di Pianosa nel Mar Tirreno Settentrionale. Atti Congresso Environment et Idendité en Mediterranée, Imprimerie Pierre-Dominique Sammarcelli, Biguglia, pp. 175–178.
Frot, E., van Wesemael, B., Vandenschrick, G., Souchez, R., Solé Benet, A., 2007. Origin and type of rainfall for recharge of a karstic aquifer in the western Mediterranean: a case study from the Sierra de Gador–Campo de Dalias (southeast Spain). Hydrol. Process. 21, 359–368. https://doi.org/10.1002/hyp.6238.
Gat, J.R., 1996. Oxygen and hydrogen isotopes in the hydrological cycle. Annu. Rev. Earth Planet. Sci. 24, 225–262. https://doi.org/10.1146/annurev.earth.24.1.225.
Gat, J.R., 2005. Some classical concepts of isotope hydrology. In: Aggarwal, P.K., Gat, Joel R., Froehlich, K.F.O. (Eds.), Isotopes in the Water Cycle: Past, Present and Future of a Developing Science. Springer, Netherlands, Dordrecht, pp. 127–137. https://doi.org/10.1007/1-4020-3023-1_10.
Gat, J.R., Mook, W.G., Meijer, H.A.J., 2001. Atmospheric water (volume II). In: Mook, W. G. (Ed.), Environmental Isotopes in the Hydrological Cycle: Principles and Applications. UNESCO IAEA, Paris.
Giorgi, F., 2002. Variability and trends of sub-continental scale surface climate in the twentieth century. Part I: observations. Clim. Dyn. 18, 675–691.
Giorgi, F., 2006. Climate change hot-spots. Geophys. Res. Lett. 33 https://doi.org/10.1029/2006GL025734.
Giorgi, F., Lionello, P., 2008. Climate change projections for the Mediterranean region. Glob. Planet. Chang. 63, 90–104. https://doi.org/10.1016/j.gloplacha.2007.09.005.
Giustini, F., Brilli, M., Patera, A., 2016. Mapping oxygen stable isotopes of precipitation in Italy. J. Hydrol. Reg. Stud. 8, 162–181. https://doi.org/10.1016/j.ejrh.2016.04.001.
Gonfiantini, R., 1986. Environmental isotopes in lake studies. In: Fritz, P., Fontes, J.C. (Eds.), Handbook of Environmental Isotope Geochemistry 2. Elsevier, New York, pp. 113–116.
Gusyev, M., Gädeke, A., Cullmann, J., Magome, J., Sugiura, A., Sawano, H., Takeuchi, K., 2016. Connecting global- and local-scale flood risk assessment: a case study of the Rhine River basin flood hazard. J. Flood Risk Manag. 9, 343–354. https://doi.org/10.1111/jfr3.12243.
Hirabayashi, Y., Mahendran, R., Koirala, S., Konoshima, L., Yamazaki, D., Watanabe, S., Kim, H., Kanae, S., 2013. Global flood risk under climate change. Nat. Clim. Chang. 3, 816–821. https://doi.org/10.1038/nclimate1911.
Hoerling, M., Eischeid, J., Perlwitz, J., Quan, X., Zhang, T., Pegion, P., 2012. On the increased frequency of Mediterranean drought. J. Clim. 25, 2146–2161. https://doi.org/10.1175/JCLI-D-11-00296.1.
Homar, V., Ramis, C., Romero, R., Alonso, S., 2010. Recent trends in temperature and precipitation over the Balearic Islands (Spain). Clim. Chang. 98, 199. https://doi.org/10.1007/s10584-009-9664-5.
Hughes, C.E., Crawford, J., 2012. A new precipitation weighted method for determining the meteoric water line for hydrological applications demonstrated using Australian and global GNIP data. J. Hydrol. 464–465, 344–351. https://doi.org/10.1016/j.jhydrol.2012.07.029.
IAEA, 2014. Precipitation Sampling Guide (V2.02). http://www-naweb.iaea.org/napc/ih/documents/other/gnip_manual_v2.02_en_hq.pdf.
IPCC, 2007. Climate change 2007: the physical science basis. In: Solomon, S., Qin, D., Manning, M., Chen, Z., Marquis, M., Averyt, K.B., Tignor, M., Miller, H.L. (Eds.), Contribution of Working Group I to the Fourth Assessment Report of the Intergovernmental Panel on Climate Change. Cambridge University Press, Cambridge, United Kingdom and New York, NY, USA.
Jasechko, S., 2019. Global isotope hydrogeology—review. Rev. Geophys. 57, 835–965. https://doi.org/10.1029/2018RG000627.
Köppen, W., 1931. Grundriß der Klimakunde. De Gruyter, Berlin, Boston. https://doi.org/10.1515/9783111667751.
Krklec, K., Domínguez-Villar, D., 2014. Quantification of the impact of moisture source regions on the oxygen isotope composition of precipitation over Eagle Cave, Central Spain. Geochim. Cosmochim. Acta 134, 39–54. https://doi.org/10.1016/j.gca.2014.03.011.
Krklec, K., Domínguez-Villar, D., Lojen, S., 2018. The impact of moisture sources on the oxygen isotope composition of precipitation at a continental site in Central Europe. J. Hydrol. 561, 810–821. https://doi.org/10.1016/j.jhydrol.2018.04.045.
Kuhn, M., 2008. Building predictive models in R using the caret Package. J. Stat. Softw. 28, 1–26. https://doi.org/10.18637/jss.v028.i05.
LeGrande, A.N., Schmidt, G.A., 2006. Global gridded data set of the oxygen isotopic composition in seawater. Geophys. Res. Lett. 33 https://doi.org/10.1029/2006GL026011.
Liotta, M., Bellissimo, S., Favara, R., Valenza, M., 2008. Isotopic composition of single rain events in the Central Mediterranean. J. Geophys. Res. Atmos. 113 https://doi.org/10.1029/2008JD009996.
Longinelli, A., Selmo, E., 2003. Isotopic composition of precipitation in Italy: a first overall map. J. Hydrol. 270, 75–88. https://doi.org/10.1016/S0022-1694(02)00281-0.
Lis, G., Wassenaar, L.I., Hendry, M.J., 2008. High-precision laser spectroscopy D/H and $^{18}O/^{16}O$ measurements of microliter natural water samples. Anal. Chem. 80, 287–293. https://doi.org/10.1021/ac701716q.
Longinelli, A., Anglesio, E., Flora, O., Iacumin, P., Selmo, E., 2006. Isotopic composition of precipitation in Northern Italy: reverse effect of anomalous climatic events. J. Hydrol. 329, 471–476. https://doi.org/10.1016/j.jhydrol.2006.03.002.
López-Moreno, J.I., Vicente-Serrano, S.M., Angulo-Martínez, M., Beguería, S., Kenawy, A., 2010. Trends in daily precipitation on the northeastern Iberian Peninsula, 1955–2006. Int. J. Climatol. 30, 1026–1041. https://doi.org/10.1002/joc.1945.
López-Moreno, J.I., Vicente-Serrano, S.M., Morán-Tejeda, E., Lorenzo-Lacruz, J., Kenawy, A., Beniston, M., 2011. Effects of the North Atlantic Oscillation (NAO) on combined temperature and precipitation winter modes in the Mediterranean mountains: Observed relationships and projections for the 21st century. Glob. Planet. Chang. 77, 62–76. https://doi.org/10.1016/j.gloplacha.2011.03.003.
Luppichini, M., Barsanti, M., Giannecchini, R., Bini, M., 2021. Statistical relationships between large-scale circulation patterns and local-scale effects: NAO and rainfall regime in a key area of the Mediterranean basin. Atmos. Res. 248, 105270 https://doi.org/10.1016/j.atmosres.2020.105270.
Luppichini, M., Bini, M., Barsanti, M., Giannecchini, R., Zanchetta, G., 2022. Seasonal rainfall trends of a key Mediterranean area in relation to large-scale atmospheric circulation: how does current global change affect the rainfall regime? J. Hydrol. 612, 128233 https://doi.org/10.1016/j.jhydrol.2022.128233.
Mathbout, S., Lopez-Bustins, J.A., Royé, D., Martin-Vide, J., 2021. Mediterranean-scale drought: regional datasets for exceptional meteorological drought events during 1975–2019. Atmosphere (Basel). 12 https://doi.org/10.3390/atmos12080941.
Milly, P.C.D., Dunne, K.A., Vecchia, A.V., 2005. Global pattern of trends in streamflow and water availability in a changing climate. Nature 438, 347–350. https://doi.org/10.1038/nature04312.
Moreno, A., Sancho, C., Bartolomé, M., Oliva-Urcia, B., Delgado-Huertas, A., Estrela, M. J., Corell, D., López-Moreno, J.I., Cacho, I., 2014. Climate controls on rainfall isotopes and their effects on cave drip water and speleothem growth: the case of Molinos cave (Teruel, NE Spain). Clim. Dyn. 43, 221–241. https://doi.org/10.1007/s00382-014-2140-6.
Natali, S., Baneschi, I., Doveri, M., Giannecchini, R., Selmo, E., Zanchetta, G., 2021. Meteorological and geographical control on stable isotopic signature of precipitation in a western Mediterranean area (Tuscany, Italy): disentangling a complex signal. J. Hydrol. 603, 126944 https://doi.org/10.1016/j.jhydrol.2021.126944.
Natali, S., Doveri, M., Giannecchini, R., Baneschi, I., Zanchetta, G., 2022. Is the deuterium excess in precipitation a reliable tracer of moisture sources and water

resources fate in the western Mediterranean? New insights from the Apuan Alps (Italy). J. Hydrol. 128497 https://doi.org/10.1016/j.jhydrol.2022.128497.
Nicotra, I., 2008. Studio idrogeologico e idrogeochimico del sistema acquifero dell'Isola di Pianosa. In: Tesi di laurea inedita. Università di Pisa.
Norrant, C., Douguédroit, A., 2006. Monthly and daily precipitation trends in the Mediterranean (1950–2000). Theor. Appl. Climatol. 83, 89–106. https://doi.org/10.1007/s00704-005-0163-y.
Numaguti, A., 1999. Origin and recycling processes of precipitating water over the Eurasian continent: experiments using an atmospheric general circulation model. J. Geophys. Res. Atmos. 104, 1957–1972. https://doi.org/10.1029/1998JD200026.
Oza, H., Padhya, V., Ganguly, A., Deshpande, R.D., 2022. Investigating hydrometeorology of the Western Himalayas: Insights from stable isotopes of water and meteorological parameters. Atmos. Res. 268, 105997 https://doi.org/10.1016/j.atmosres.2021.105997.
Pastor, F., Valiente, J.A., Palau, J.L., 2018. Sea Surface Temperature in the Mediterranean: Trends and Spatial patterns (1982–2016). Pure Appl. Geophys. 175, 4017–4029. https://doi.org/10.1007/s00024-017-1739-z.
Penna, D., Hopp, L., Scandellari, F., Allen, S.T., Benettin, P., Beyer, M., Geris, J., Klaus, J., Marshall, J.D., Schwendenmann, L., Volkmann, T.H.M., von Freyberg, J., Amin, A., Ceperley, N., Engel, M., Frentress, J., Giambastiani, Y., McDonnell, J.J., Zuecco, G., Llorens, P., Siegwolf, R.T.W., Dawson, T.E., Kirchner, J.W., 2018. Ideas and perspectives: tracing terrestrial ecosystem water fluxes using hydrogen and oxygen stable isotopes – challenges and opportunities from an interdisciplinary perspective. Biogeosciences 15, 6399–6415. https://doi.org/10.5194/bg-15-6399-2018.
Pfahl, S., Sodemann, H., 2014. What controls deuterium excess in global precipitation? Clim. Past 10, 771–781. https://doi.org/10.5194/cp-10-771-2014.
R Core Team, 2019. R: A Language and Environment for Statistical Computing. R Foundation for Statistical Computing, Vienna, Austria. https://www.R-project.org/.
Raggi, G., 1983. Le acque del sottosuolo dell'Isola di Pianosa. Atti Soc. Tosc. Sc. Nat., Mem., Serie A 90, 75–84.
Reale, M., Lionello, P., 2013. Synoptic climatology of winter intense precipitation events along the Mediterranean coasts. Nat. Hazards Earth Syst. Sci. 13, 1707–1722. https://doi.org/10.5194/nhess-13-1707-2013.
Revelle, W., 2023. Psych: Procedures for Psychological, Psychometric, and Personality Research. Northwestern University, Evanston, Illinois. R package version 2.3.3. https://CRAN.R-project.org/package=psych.
Rindsberger, M., Magaritz, M., Carmi, I., Gilad, D., 1983. The relation between air mass trajectories and the water isotope composition of rain in the Mediterranean Sea area. Geophys. Res. Lett. 10, 43–46. https://doi.org/10.1029/GL010i001p00043.
Rolph, G., Stein, A., Stunder, B., 2017. Real-time Environmental applications and Display sYstem: READY. Environ. Model. Softw. 95, 210–228. https://doi.org/10.1016/j.envsoft.2017.06.025.
Rozanski, K., Araguás-Araguás, L., Gonfiantini, R., 1993. Isotopic patterns in global precipitation. J. Geophys. Res. 78 https://doi.org/10.1029/GM078p0001.
Saranya, P., Krishnakumar, A., Sinha, N., Kumar, S., Anoop Krishnan, K., 2021. Isotopic signatures of moisture recycling and evaporation processes along the Western Ghats orography. Atmos. Res. 264, 105863 https://doi.org/10.1016/j.atmosres.2021.105863.
Sodemann, H., Schwierz, C., Wernli, H., 2008. Interannual variability of Greenland winter precipitation sources: Lagrangian moisture diagnostic and North Atlantic Oscillation influence. J. Geophys. Res. Atmos. 113 https://doi.org/10.1029/2007JD008503.
Spearman, C., 1904. The Proof and Measurement of Association between two things. Am. J. Psychol. 15, 72–101. https://doi.org/10.2307/1412159.
Stein, A.F., Draxler, R.R., Rolph, G.D., Stunder, B.J.B., Cohen, M.D., Ngan, F., 2015. NOAA's HYSPLIT Atmospheric Transport and Dispersion Modeling System. Bull. Am. Meteorol. Soc. 96, 2059–2077. https://doi.org/10.1175/BAMS-D-14-00110.1.
Toreti, A., Xoplaki, E., Maraun, D., Kuglitsch, F.G., Wanner, H., Luterbacher, J., 2010. Characterisation of extreme winter precipitation in Mediterranean coastal sites and associated anomalous atmospheric circulation patterns. Nat. Hazards Earth Syst. Sci. 10, 1037–1050. https://doi.org/10.5194/nhess-10-1037-2010.
Trenberth, K.E., 2011. Changes in precipitation with climate change. Clim. Res. 47, 123–138. https://doi.org/10.3354/cr00953.
Turco, M., Palazzi, E., von Hardenberg, J., Provenzale, A., 2015. Observed climate change hotspots. Geophys. Res. Lett. 42, 3521–3528. https://doi.org/10.1002/2015GL063891.
Uemura, R., Matsui, Y., Yoshimura, K., Motoyama, H., Yoshida, N., 2008. Evidence of deuterium excess in water vapor as an indicator of ocean surface conditions. J. Geophys. Res. Atmos. 113 https://doi.org/10.1029/2008JD010209.
Unesco, 1991. Hydrology and Water Resources of Small Islands: a Practical Guide.
Wallance, J., Hobbs, P., 2006. Atmospheric Science: An Introductory Survey. Academic, San Diego.
Warner, M.S.C., 2018. Introduction to PySPLIT: a Python Toolkit for NOAA ARL's HYSPLIT Model. Comput. Sci. Eng. 20, 47–62. https://doi.org/10.1109/MCSE.2017.3301549.
Watanabe, T., Cullmann, J., Pathak, C.S., Turunen, M., Emami, K., Ghinassi, G., Siddiqi, Y., 2018. Management of climatic extremes with focus on floods and droughts in agriculture. Irrig. Drain. 67, 29–42. https://doi.org/10.1002/ird.2204.
Wickham, H., 2011. The split-apply-combine strategy for data analysis. J. Stat. Softw. 40, 1–29. https://www.jstatsoft.org/v40/i01/.
Wickham, H., Averick, M., Bryan, J., Chang, W., McGowan, L., François, R., Grolemund, G., Hayes, A., Henry, L., Hester, J., Kuhn, M., Pedersen, T., Miller, E., Bache, S., Müller, K., Ooms, J., Robinson, D., Seidel, D., Spinu, V., Takahashi, K., Vaughan, D., Wilke, C., Woo, K., Yutani, H., 2019. Welcome to the tidyverse. J. Open Source Softw. 4, 1686. https://doi.org/10.21105/joss.01686.
Wolf, A., Roberts, W.H.G., Ersek, V., Johnson, K.R., Griffiths, M.L., 2020. Rainwater isotopes in Central Vietnam controlled by two oceanic moisture sources and rainout effects. Sci. Rep. 10, 16482. https://doi.org/10.1038/s41598-020-73508-z.
Xia, Z., Winnick, M.J., 2021. The competing effects of terrestrial evapotranspiration and raindrop re-evaporation on the deuterium excess of continental precipitation. Earth Planet. Sci. Lett. 572, 117120 https://doi.org/10.1016/j.epsl.2021.117120.
Xiang, Q., Liu, G., Meng, Y., Chen, K., Xia, C., 2022. Temporal trends of deuterium excess in global precipitation and their environmental controls under a changing climate. J. Radioanal. Nucl. Chem. 331, 3633–3649. https://doi.org/10.1007/s10967-022-08414-x.
Xoplaxi, E., 2002. Climate Variability over the Mediterranean. PhD Thesis. University of Bern, Switzerland. Available through. http://sinus.unibe.ch/klimet/docs/phd_xoplaki.pdf.
Zhang, J., Genty, D., Sirieix, C., Michel, S., Minster, B., Régnier, E., 2020. Quantitative assessments of moisture sources and temperature governing rainfall δ18O from 20 years' monitoring records in SW-France: importance for isotopic-based climate reconstructions. J. Hydrol. 591, 125327 https://doi.org/10.1016/j.jhydrol.2020.125327.
Zhao, J., Tan, L., Li, D., Pérez-Mejías, C., Dong, X., Wang, J., Zhang, H., Cheng, H., 2022. The seasonally Altered Atmosphere Moisture Circulations with Rainfall and Rainfall Isotopes in Southwest China. Front. Earth Sci. 10 https://doi.org/10.3389/feart.2022.795857.